Anticancer Chemotherapy Inhibits MHC Class I–Related Chain A Ectodomain Shedding by Downregulating ADAM10 Expression in Hepatocellular Carcinoma

Keisuke Kohga, Tetsuo Takehara, Tomohide Tatsumi, Takuya Miyagi, Hisashi Ishida, Kazuyoshi Ohkawa, Tatsuya Kanto, Naoki Hiramatsu, and Norio Hayashi

Department of Gastroenterology and Hepatology, Osaka University Graduate School of Medicine, Osaka, Japan

Abstract

MHC class I–related chain A (MICA) is a ligand for the NKG2D-activating immunoreceptor that mediates activation of natural killer (NK) cells. The ectodomain of MICA is shed from tumor cells, which may be an important means of evading antitumor immunity. We previously reported that patients with hepatocellular carcinoma (HCC) display high levels of soluble MICA in circulation, which could be downregulated by chemotherapy. The present study shows that anti-HCC drugs suppress MICA ectodomain shedding by inhibiting expression of a disintegrin and metalloproteinase 10 (ADAM10). Both ADAM10 and CD44, a typical substrate of the ADAM10 protease, were expressed in human HCC tissues and HCC cells but not in normal liver tissues or cultured hepatocytes. Small interfering RNA–mediated knockdown experiments revealed that ADAM10 is a critical sheddase for both MICA and CD44 in HCC cells. Of interest is the finding that epirubicin clearly downregulated ADAM10 expression and MICA shedding in HCC cells; its suppressive effect on MICA shedding was abolished in ADAM10-depleted cells. Epirubicin treatment also enhanced the NKG2D-mediated NK sensitivity of HCC cells. Patients with HCC had significantly higher levels of serum-soluble CD44, which correlated well with serum-soluble MICA levels, thus suggesting a close link between ADAM10 activity and MICA shedding in these patients. Soluble MICA and CD44 levels were downregulated with a significant correlation in patients treated by transarterial chemoembolization using epirubicin. In conclusion, anticancer drugs can modulate expression of ADAM10, which is critically involved in MICA ectodomain shedding. Epirubicin therapy may have a previously unrecognized effect on antitumor immunity in HCC patients. [Cancer Res 2009;69(20):8050–7]

Introduction

Hepatocellular carcinoma (HCC) is one of the leading causes of cancer deaths worldwide. Chronic liver disease caused by hepatitis virus infection and nonalcoholic steatohepatitis leads to a predisposition for HCC, with liver cirrhosis, in particular, being considered a premalignant condition (1, 2). With regard to treatment, surgical resection or percutaneous techniques such as ethanol injection and radiofrequency ablation are considered to be choices for curable treatment of localized HCC, whereas transcatheter arterial chemoembolization (TACE) is a well-established technique for more advanced HCC (3). The liver contains a large compartment of innate immune cells [natural killer (NK) cells and natural killer T cells] and acquired immune cells (T cells; refs. 4, 5), but the activation of these immune cells after HCC treatments remains unclear. If such treatments can efficiently activate abundant immune cells in the liver, this could lead to the establishment of attractive new strategies for HCC treatment.

MHC class I–related chain A and B (MICA and MICB) are ligands for NKG2D expressed on a variety of immune cells (6). In contrast to classic MHC class I molecules, MICA/B are rarely expressed on normal cells but frequently on tumor cells (7–10). The engagement of MICA/B and NKG2D strongly activates NK cells and costimulates T cells, enhancing their cytolytic activity and cytokine production (11). Thus, the MICA/B-NKG2D pathway is an important mechanism by which the host immune system recognizes and kills transformed cells (12). In addition to those membrane-bound forms, MICA/B molecules are also cleaved proteolytically from tumor cells and appear as soluble forms in sera of patients with malignancy (13–15). Soluble MICA/B in circulation downregulates NKG2D expression and disturbs NKG2D-mediated antitumor immunity (9, 10, 13). We previously reported that soluble MICA could be detected in sera of HCC patients (16) and that TACE treatment reduces the levels of soluble MICA and thereby upregulates the expression of NKG2D (17). Thus, cancer therapy may have a beneficial effect on NKG2D-mediated immune responses.

The release of soluble MICA/B from tumor cells is impaired by metalloproteinase inhibitors, suggesting the involvement of members of the metzincin superfamily, such as ADAM proteins (14, 18). In addition, ERp5, related to protein disulfide isomerase, is required for the MICA shedding as it reduces disulfide bond of the α3 domain of MICA (19). Although it may not be a direct protease for MICA, it may enable proteolytic cleavage through conformational change. Recently, it was reported that MICA shedding of 293T fibroblast cells and HeLa cervical cancer cells was inhibited by silencing of the ADAM10 and ADAM17 proteases (20). This suggests that ADAM family proteins may be a therapeutic target for enhancing antitumor immunity, but how to therapeutically modulate these proteins is still not clear. Furthermore, it remains to be determined whether ADAMs can regulate MICA shedding in a clinical setting.

In the present study, we showed that ADAM10, but not ADAM17, was critically required for MICA shedding in human HCC cells. Of importance is the discovery that epirubicin, a widely used anti-HCC drug, was capable of downregulating ADAM10 expression and

Note: Supplementary data for this article are available at Cancer Research Online (http://cancerres.aacrjournals.org/).

K. Kohga, T. Takehara, and T. Tatsumi contributed equally to this work.

Requests for reprints: Norio Hayashi, Department of Gastroenterology and Hepatology, Osaka University Graduate School of Medicine, 2-2 Yamadaoka, Suita, Osaka 565-0871, Japan. Phone: 81-6-6879-3621; Fax: 81-6-6879-3629; E-mail: hayashin@gh.med.osaka-u.ac.jp.

doi:10.1158/0008-5472.CAN-09-0789

activity in HCC cells; it can thus inhibit MICA shedding and enhance NK sensitivity. ADAM10 was immunohistochemically detected in HCC tissues and a correlation was observed between soluble MICA levels and ADAM10 activity determined by soluble CD44 levels in HCC patients. The present study sheds light on previously unrecognized effects of an anticancer drug on modulating ADAM family proteins and MICA shedding and thus suggests a promising aspect for chemoimmunotherapy against human HCC.

Materials and Methods

Liver tissues and immunohistochemistry. Human HCC tissues (n = 8) and normal liver tissues (n = 2) obtained at surgical resection were used. Informed consent, under an institutional review board–approved protocol,

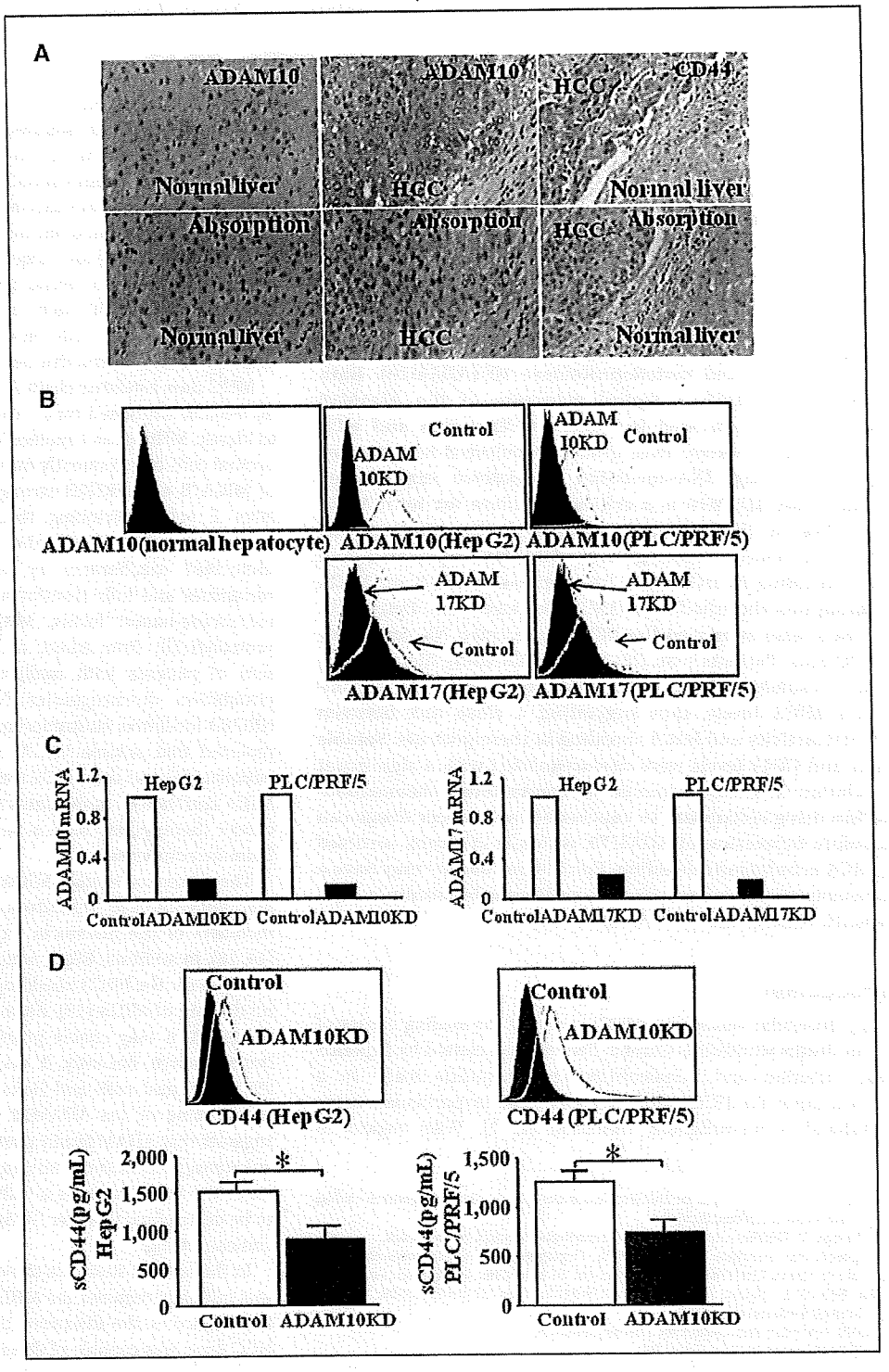

Figure 1. Expression of ADAM10 and CD44 in human HCC tissues and ADAM10 or ADAM17 knockdown in human HCC cells. *A*, immunohistochemical detection of ADAM10 and CD44 in human HCC tissues (n = 8) and normal liver tissues (n = 2). Liver sections were stained with the corresponding antibodies (*top panels*). Both primary antibodies were incubated with recombinant CD44 and ADAM10 proteins and then applied to liver sections in parallel as the absorption test (*bottom panels*). Representative images are shown. *B* and *C*, expression of ADAM10 or ADAM17 in human primary hepatocyte and HCC cell lines (*HepG2* and *PLC/PRF/5*). Cells were treated with ADAM10 siRNA, ADAM17 siRNA, or control siRNA, and subjected to analysis of ADAM10 or ADAM17 expression by flow cytometry (*B*) or real-time RT-PCR (*C*). *Histograms*, anti-ADAM10 or anti-ADAM17 staining of ADAM10 or ADAM17 siRNA-treated cells (*ADAM10KD* or *ADAM17KD, black dotted line*) and control siRNA-treated cells (*Control, gray line*), respectively. *Closed histograms*, control IgG staining. *D*, the expression of membrane-bound CD44 on HCC cells treated with ADAM10 siRNA (ADAM10KD, *black line*) or control siRNA (*Control, gray line*) was evaluated by flow cytometry (*top panels*). *Closed histograms*, control IgG staining. Soluble CD44 (*sCD44*) production from HCC cells treated with ADAM10 siRNA or control siRNA were evaluated by specific ELISA (*bottom panels*). *, $P < 0.05$.

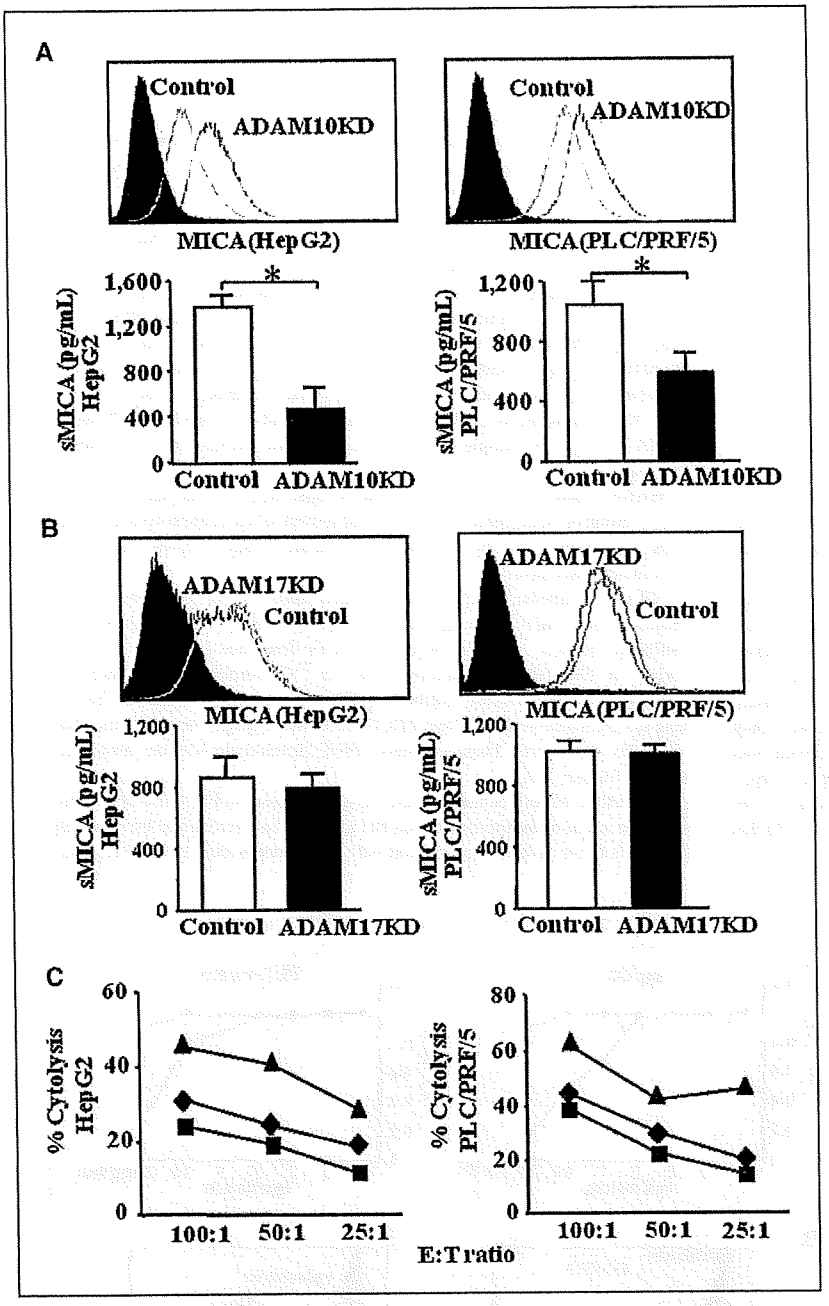

Figure 2. Expression of MICA in ADAM10 or ADAM17 knockdown HCC cells and NK sensitivity in ADAM10 knockdown HCC cells. *A* and *B*, the expression of membrane-bound MICA on HCC cells treated with ADAM10 siRNA (*ADAM10KD, black line*; *A*), ADAM17 siRNA (*ADAM17KD, black line*; *B*), or control siRNA (*Control, gray line*) was evaluated by flow cytometry (*top panels*). *Closed histograms*, control IgG staining. Soluble MICA (*sMICA*) production from HCC cells treated with ADAM10 siRNA (*A*), ADAM17 siRNA (*B*), or control siRNA were evaluated by specific ELISA (*bottom panels*). *, $P < 0.05$. *C*, HCC cells treated with ADAM10 siRNA or control siRNA were subjected to ^{51}Cr-release assay against NK cells. Cytolytic activity of NK cells against control HCC cells (■) or ADAM10 knockdown HCC cells without (▲) or with blocking antibody of MICA/B (6D4; ♦). Representative results are shown. Similar results were obtained from three independent experiments.

was obtained from all patients before sample acquisition. Liver sections were subjected to immunohistochemical staining using the ABC procedure (Vector Laboratories, Burlingame, CA). The primary antibodies used were anti-ADAM10 and anti-CD44 (R&D Systems). To confirm the specificity of the staining, primary antibodies were incubated with recombinant CD44 or ADAM10 protein (R&D Systems, Minneapolis, MN) for 3 h and then applied onto liver sections in parallel with staining of the primary antibodies as the absorption test.

HCC cell lines. Human HCC cell lines HepG2 and PLC/PRF/5 were purchased from the American Type Culture Collection and were cultured with DMEM supplemented with 10% fetal bovine serum (GIBCO/Life Technologies, Grand Island, NY) in a humidified incubator at 5% CO_2 and 37°C.

RNA silencing. The small interfering RNA (siRNA) method was used to knockdown ADAM10 and ADAM17. Stealth RNAi oligonucleotide targeting ADAM10 or ADAM17 and scrambled oligonucleotides as a control were purchased from Invitrogen (Carlsbad, CA). Cells were transfected by RNAi Max transfection reagent (Invitrogen) with 50 nmol/L siRNA. At 24 h posttransfection, the cells were analyzed for specific depletion of the mRNAs of ADAM10 and ADAM17 by real-time reverse transcription-PCR (RT-PCR; Applied Biosystems, Foster City, CA). The following siRNAs were used: ADAM10, 5′-AUAUCUGGGCAAUCACAG-CUUCUCG-3′; scramble control, 5′-AUACUUGGUCAACGCACUUCGAUGG-3′; ADAM17, 5′-UGAACAAGCUCUUCAGGUGGUUCUC-3′; scramble control, 5′-UGAUUAGAACUCUCGACUGGUGCUC-3′.

ELISA. The supernatants of cultured cells were harvested at 24 h after transfection with siRNA as well as sera from HCC patients ($n = 97$) and age-matched healthy volunteers ($n = 32$) were subjected to analysis of soluble MICA and soluble CD44 levels. Informed consent, under an institutional review board–approved protocol, was obtained from all patients before sample acquisition. The levels of soluble MICA and soluble CD44 were

determined by DuoSet MICA eELISA kit (R&D Systems) and soluble CD44std ELISA (Abcam, Cambridge, MA), respectively.

Flow cytometry. For the detection of membrane-bound MICA and CD44, cells were incubated with an anti-MICA–specific antibody (2C10, Santa Cruz Biotechnology, Santa Cruz, CA) or anti-CD44 antibody (R&D Systems) and stained with phycoerythrin (PE)-goat anti-mouse immunoglobulin (Beckman Coulter) as a secondary reagent and then subjected to flow cytometric analysis. For the detection of ADAM10 or ADAM17, cells were fixed and permeabilized with Cytofix/Cytoperm (BD Biosciences, San Jose, CA) and stained with PE-conjugated anti-ADAM10 or anti-ADAM17 antibody (R&D Systems). Flow cytometric analysis was performed using a FACScan flow cytometer (Becton Dickinson).

Plasmid construction of pMyc-MICA. MICA full coding cDNA was isolated from Huh7, human HCC cells, using a conventional RT-PCR method (Supplementary Fig. S1, DDBJ/EMBL/Genbank accession number AB506764) and inserted into the *Hin*dIII-*Xba*I site of pcDNA3 (Invitrogen). A C-myc tag was placed between the leader peptide and the α1 domain of MICA by site-specific mutagenesis using a QuikChange site-directed mutagenesis kit (Stratagene, La Jolla, CA) referred to as pMyc-MICA. Cells were transfected with pMyc-MICA using a Lipofectamine LTX reagent (Invitrogen). The green fluorescent protein (GFP)–expressing vector (pEGFP-C1, Clontech, Mountain View, CA) was cotransfected to evaluate the transfection efficiency.

Immunoprecipitation. Cells or tissues were homogenized in lysis buffer containing 1% NP40, 0.5% sodium deoxycholate, 0.1% SDS, 50 μg/mL aprotinin, 100 μg/mL phenylmethylsulfonyl fluoride, 1 mmol/L sodium orthovanadate, 50 mmol/L sodium fluoride, and PBS. To the cell supernatants, 0.5% NP40 and a cocktail of protease inhibitors were added. The protein contents of the samples were determined by BCA protein assay kit (Pierce, Rackford, IL). Immunoprecipitation with anti–c-Myc beads was performed for 1 h at 4°C. Immunocomplexes were eluted by a c-Myc–tagged peptide solution (MBL, Woburn, MA). The samples after immunoprecipitation were treated with 250 mU of N-glycosidase F (Roche, Mannheim, Germany) for 3 h at 37°C.

Western blotting. The total cellular protein was electrophoretically separated using SDS-12% polyacrylamide gels and transferred onto polyvinylidene difluoride membrane. The membrane was blocked in TBS-Tween containing 5% skim milk for 1 h and then probed with anti-Myc mouse monoclonal antibody (Cell Signaling Technology, Danvers, MA) at 4°C overnight. Horseradish peroxidase–conjugated anti-rabbit antibody and SuperSignal West Pico System (Pierce) were used for the detection of blots.

Real-time RT-PCR. Total RNA was isolated using RNeasy Mini Kit (Qiagen K.K., Tokyo, Japan) and was reverse transcribed using SuperScript III First-Strand Synthesis System (Invitrogen). The mRNA levels were evaluated using ABI PRISM 7900 Sequence Detection System (Applied Biosystems). Ready-to-use assays (Applied Biosystems) were used for the quantification of ADAM10 (Hs00153853_m1), ADAM17 (Hs00234221_m1), MICA (Hs00792195_m1), β-actin (Hs99999903_m1), and CD44 (Hs00174139_m1) mRNAs according to the manufacturer's instructions. The thermal cycling conditions for all genes were 2 min at 50°C and 10 min at 95°C, followed by 40 cycles at 95°C for 15 s and 60°C for 1 min. β-Actin mRNA from each sample was quantified as an endogenous control of internal RNA.

WST-8 assay. HepG2 and PLC/PRF/5 cells were treated with different concentrations of epirubicin for 24 h. Cell growth of epirubicin-treated HCC cells was determined by WST-8 assay (Nacalai Tesque, Kyoto, Japan) as previously described (21).

NK cell analysis. NK cells were isolated from human peripheral blood mononuclear cells by magnetic cell sorting using CD56 MicroBeads (Miltenyl Biotech, Auburn, CA) as previously described (16). The cytolytic ability of NK cells was assessed by 4-h ^{51}Cr-releasing assay with or without MICA/B-blocking antibody (6D4; ref. 7), which binds to the α1 and α2 domains of MICA and MICB. 6D4 was a generous gift from Drs. Veronika Groh and Thomas Spies (Fred Hutchinson Cancer Research Center, Seattle, WA).

Statistics. All values were expressed as the mean and SD. The statistical significance of differences between the groups was determined by applying Student's *t* test or two-sample *t* test with Welch correction after each group

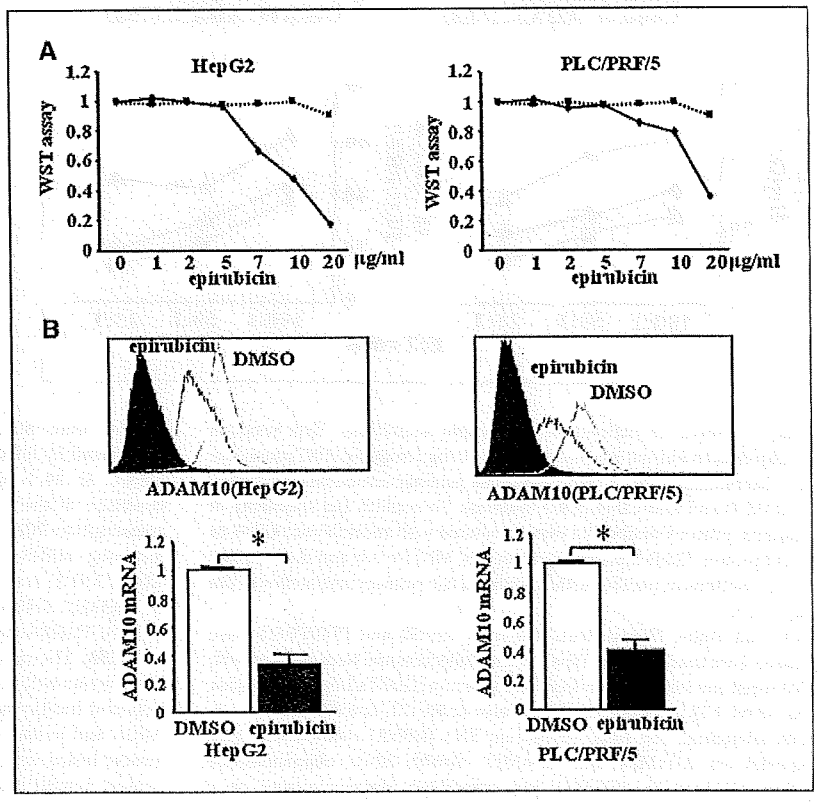

Figure 3. Expression of ADAM10 in epirubicin-treated HCC cells. *A*, the cytotoxicity of epirubicin to human HCC cells was evaluated by WST-8 assay. Cells were treated with different doses of epirubicin (*solid lines*) or vehicle (*DMSO*; *dotted lines*) for 24 h, and the viability of the cells was evaluated by the WST-8 assay. *B*, ADAM10 expression of epirubicin-treated HCC cells. Cells were treated with a nontoxic dose of 1 μg/mL epirubicin (*black lines*) or vehicle (DMSO, *gray lines*) for 24 h and their ADAM10 expression was evaluated by flow cytometry (*top panels*). *Closed histograms*, control IgG staining. Total RNA was extracted at 24 h of epirubicin treatment and mRNA levels of ADAM10 were evaluated by real-time RT-PCR (*bottom panels*). *, $P < 0.05$.

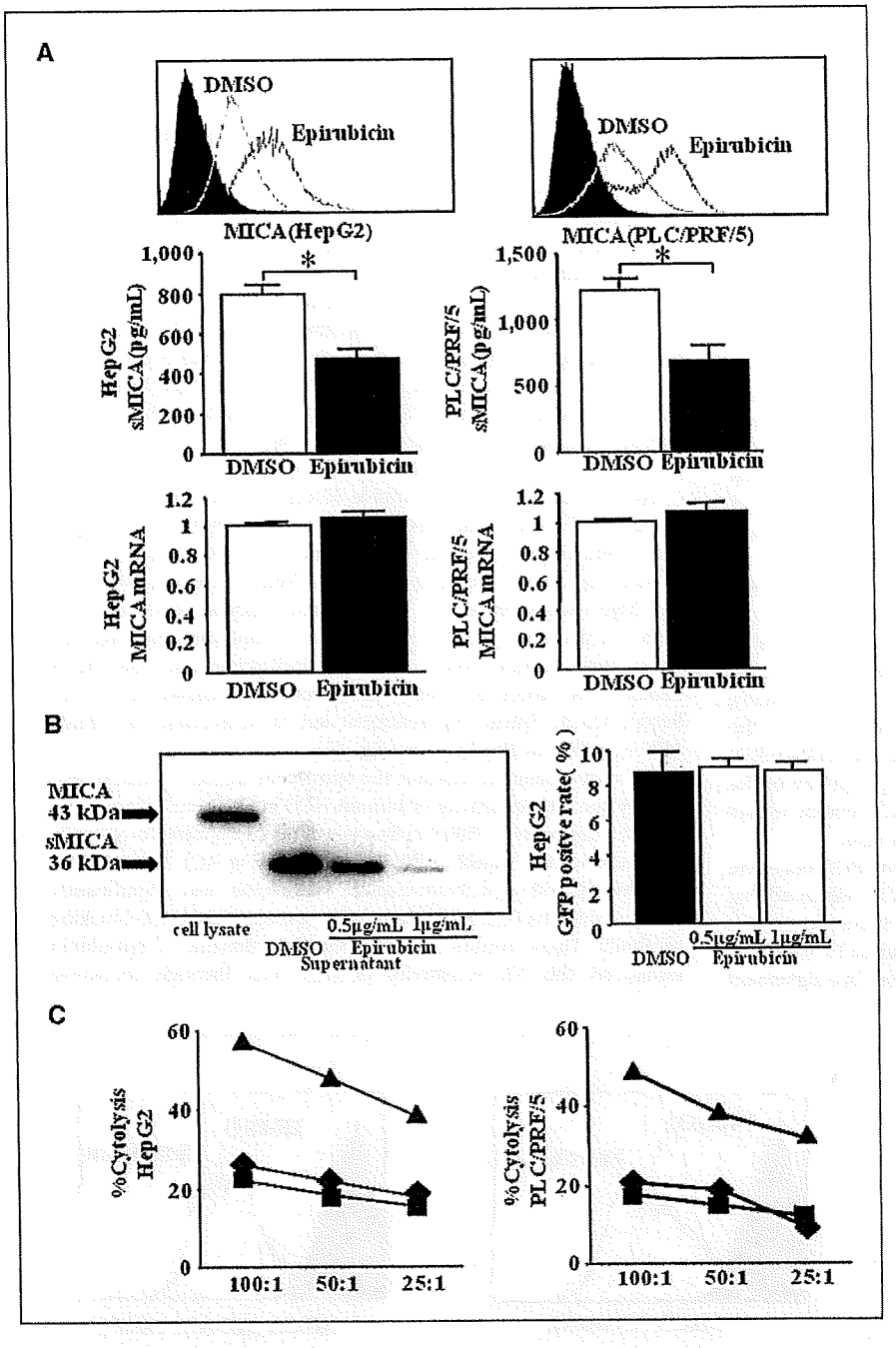

Figure 4. Expression and shedding of MICA in epirubicin-treated HCC cells. *A*, HCC cells were treated with a nontoxic dose of 1 μg/mL epirubicin (*black lines*) or vehicle (DMSO, *gray lines*) for 24 h and their expression of membrane-bound MICA and MICA mRNA was evaluated by flow cytometry (*top panels*) and real-time RT-PCR (*bottom panels*), respectively. *Closed histograms*, control IgG staining in flow cytometry. At the same time, 24-h culture supernatants were subjected to the analysis of soluble MICA (*sMICA*) levels by ELISA (*middle panels*). *, $P < 0.05$. *B*, HepG2 cells were transfected with pMyc-MICA and pEGFP-C1, cultured with 0.5 to 1 μg/mL epirubicin or vehicle (DMSO) for 24 h. Cell lysates from HepG2 cells and 24-h culture supernatants of epirubicin- or vehicle-treated HepG2 cells were immunoprecipitated with anti-Myc. The resulting immunoprecipitates were eluted, treated with N-glycanase, and subjected to Western blot analysis for MICA (*left*). Transfection efficacies were equal in all treatment groups as evidenced by similar GFP-positive cell rates (*right*). *C*, the cytolytic activity of NK cells against HCC cells. Vehicle-treated cells (■) or epirubicin-treated cells without (▲) or with blocking antibody of MICA/B (6D4; ♦) were subjected to ^{51}Cr-release assay. Representative results are shown. Similar results were obtained from three independent experiments.

had been tested with equal variance and Fisher's exact probability test. We defined statistical significance as $P < 0.05$.

Results

ADAM10 and CD44 are overexpressed in human HCC. ADAM10 was detected in all human HCC tissues tested by immunohistochemistry but not in normal liver tissues (Fig. 1*A*). Flow cytometric analysis revealed that ADAM10 was strongly expressed in a variety of HCC cell lines, including HepG2, PLC/PRF/5 (depicted in Fig. 1*B*), and Hep3B (data not shown), but faintly in primary hepatocytes. CD44, a typical substrate of the ADAM10 protease, was also expressed in all human HCC tissues but not in normal liver tissues (Fig. 1*A*). The data suggest that overexpression of ADAM10 and CD44 is a characteristic of human HCC like other malignancies (22).

ADAM10 is involved in MICA shedding of HCC cells but ADAM17 is not. To examine the involvement of ADAM family proteins in MICA ectodomain shedding, ADAM10 or ADAM17 were knocked down in HCC cells using a siRNA-mediated procedure. ADAM10 expression was clearly suppressed in HepG2 cells and PLC/PRF/5 cells at both mRNA and protein levels (Fig. 1*B* and *C*). Both cell lines expressed CD44 on the cellular surface and produced significant levels of soluble CD44 (Fig. 1*D*), indicating that CD44 is expressed and shed from those cell lines. ADAM10 knockdown (KD)

led to an increase in CD44 expression on HCC cells and a decrease in soluble CD44 levels in culture supernatants (Fig. 1*D*). Because ADAM10 has been established as being a sheddase for CD44, siRNA-mediated knockdown of ADAM10 suppressed not only the expression but also the activity of ADAM10 in HCC cells. HepG2 and PLC/PRF/5 cells also expressed ADAM17, which was clearly knocked down by a siRNA-mediated procedure (Fig. 1*B*).

HepG2 cells and PLC/PRF/5 cells expressed membrane-bound MICA and also produced soluble MICA (Fig. 2*A*). Knockdown of ADAM10 for both cell lines clearly upregulated MICA expression on their cellular surface and downregulated soluble MICA levels in their culture supernatant (Fig. 2*A*). In contrast, knockdown of ADAM17 did not affect the expression of membrane-bound MICA or the production of soluble MICA (Fig. 2*B*). We also examined the involvement of ADAM17 in MICA shedding of phorbol 12-myristate 13-acetate (PMA)–stimulated HCC cells because ADAM17 is considered to primarily affect stimulated shedding. The expression of membrane-bound MICA and the soluble MICA production were equal between PMA-stimulated ADAM17KD-HCC cells and control HCC cells (Supplementary Fig. S2). Thus, ADAM10, but not ADAM17, is critically involved in the shedding of MICA in HCC cells.

We next evaluated the cytolytic activity of NK cells against HCC cells. The cytolytic activity of NK cells against ADAM10KD-HepG2 cells was higher than that against control HepG2 cells. This activity was inhibited by blocking of anti-MICA/B antibody, suggesting that the increase of NK sensitivity depended on the increased expression of membrane-bound MICA on ADAM10KD-HepG2 cells, although we could not exclude the possibility of the involvement of MICB in this cytotoxicity (Fig. 2*C*). Similar results were also obtained with ADAM10KD-PLC/PRF/5 cells.

Epirubicin suppresses ADAM10 expression in HCC cells. We examined the biological modification of human HCC cells by adding epirubicin, which is commonly used in anti-HCC chemotherapy. We first examined the cytotoxicity of epirubicin to human HCC cells by WST-8 assay. Adding >5 μg/mL of epirubicin resulted in a significant decrease in cell growth of both HepG2 and PLC/PRF/5 cells (Fig. 3*B*). Based on these findings, we used 1 μg/mL of epirubicin to evaluate the biological effect on human HCC cells without toxicity. Both HepG2 cells and PLC/PRF/5 cells were cultured for 24 h with epirubicin and then subjected to analysis of ADAM10 expression. Epirubicin suppressed ADAM10 expression at the mRNA and protein levels in both cell lines (Fig. 3*C*). Although the data are not shown, doxorubicin also suppressed ADAM10 expression in HCC cells.

Epirubicin inhibits MICA ectodomain shedding and enhances susceptibility to NK cells of HCC cells. The above observations led us to investigate whether epirubicin or doxorubicin treatment would affect MICA ectodomain shedding in HCC cells. Epirubicin treatment led to an increase in membrane-bound MICA expression and a decrease in soluble MICA production in both HepG2 and PLC/PRF/5 cells (Fig. 4*A*). The mRNA levels of MICA did not change after exposure to epirubicin in both HCC cells (Fig. 4*A*). Similar data were obtained with doxorubicin-treated cells (data not shown).

To confirm whether the soluble MICA detected by ELISA was actually reflected in the cleaved form, we transfected Myc-tagged MICA into HepG2 cells and collected culture supernatants as well as cellular lysates. Immunprecipitates from these samples with anti-Myc were subjected to Western blot analysis after treatment with N-glycosidase. MICA in the culture supernatants migrated faster than cellular MICA (Fig. 4*B*), indicating that the MICA detected by ELISA is actually processed and released from full-length MICA. Epirubicin treatment led to a decrease in soluble MICA protein in HepG2 cells (Fig. 4*B*).

We next evaluated whether the epirubicin treatment could also modify the NK sensitivity of human HCC cells. Epirubicin-treated HepG2 cells or PLC/PRF/5 cells were more susceptible to NK cells than nontreated HepG2 or PLC/PRF/5 cells (Fig. 4*C*). The cytolytic activity against epirubicin-treated HCC cells was significantly decreased to the control levels by adding the anti-MICA/B blocking antibody. These results showed that the addition of epirubicin enhanced the NK sensitivity of HCC cell through increased

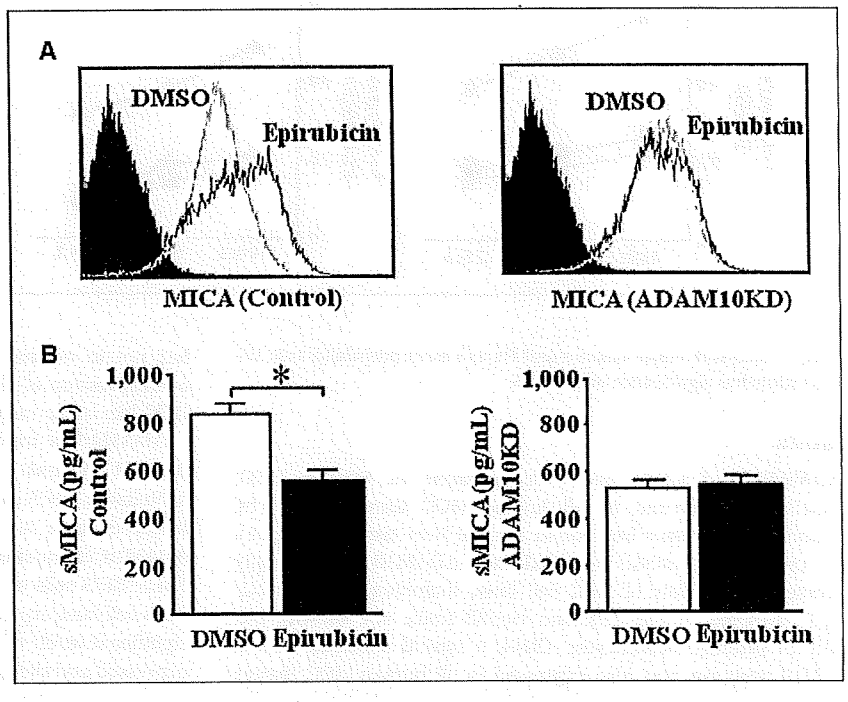

Figure 5. The epirubicin-mediated modification of MICA is ADAM10 dependent. HepG2 cells were transfected with ADAM10 siRNA (*ADAM10KD*) or control siRNA (*Control*) and further cultured with 1 μg/mL of epirubicin (*black lines*) or vehicle (DMSO, *gray line*) for 24 h. The expression of membrane-bound MICA (*MICA*) was evaluated by flow cytometry (*A*), and the soluble MICA (*sMICA*) production in the culture supernatant was evaluated by specific ELISA (*B*). Similar results were obtained from two independent experiments. *, $P < 0.05$.

expression of membrane-bound MICA, although the possibility of MICB involvement could not be excluded. The doxorubicin-treated human HCC cells showed similar results to those obtained from epirubicin-treated HCC cells (data not shown).

Epirubicin inhibits MICA ectodomain shedding through suppression of ADAM10. To examine whether the suppressive effect of epirubicin on MICA shedding occurred through downregulation of ADAM10, HepG2 cells were transfected with ADAM10 siRNA or scramble siRNA as a control and then treated with epirubicin. Consistent with earlier observations, epirubicin upregulated MICA surface expression and downregulated the levels of soluble MICA in control cells (Fig. 5). In contrast, neither upregulation of surface MICA nor downregulation of soluble MICA levels was observed in ADAM10KD-HepG2 cells. These results suggest that the suppressive effect of epirubicin on MICA shedding is mediated by ADAM10 downregulation. We also found similar results with ADAM10KD-PLC/PRF/5 cells (data not shown).

Soluble CD44 and soluble MICA levels in patients with HCC. We have shown that ADAM10 is expressed in human HCC tissues. However, it is not clear whether ADAM10 activity in HCC tissues is actually involved in MICA shedding in patients. Because ADAM10 was reported to be the constitutive functional sheddase of CD44 (23), we examined the soluble CD44 levels in HCC patients, which might be produced from tumor cells through ADAM10 activity. As shown in Fig. 6*A*, the soluble CD44 levels in HCC patients (n = 97) were significantly higher than those in age-matched healthy volunteers (n = 32). More importantly, soluble MICA levels in HCC patients significantly correlated with soluble CD44 levels (Fig. 6*B*), suggesting a close link between MICA shedding and ADAM10 activity.

We further examined soluble CD44 levels before and 2 weeks after TACE in HCC patients. Whereas the levels did not change in nontreated HCC patients during the 2-week interval (n = 9; 306.7 ± 82.5 ng/mL and 309.9 ± 79.9 ng/mL after 2 weeks), they were significantly decreased in epirubicin-based TACE-treated HCC patients (n = 21; 339.7 ± 78.1 ng/mL before TACE and 308.9 ± 81.4 ng/mL after TACE, P < 0.003). The changes of soluble CD44 in TACE treatment correlated significantly with those of soluble MICA (P = 0.0002; Fig. 6*C*). These results indicated that ADAM10-mediated CD44 shedding was decreased after TACE in HCC patients, implying that this reduction of ADAM10 activity might be related to the decline in MICA shedding.

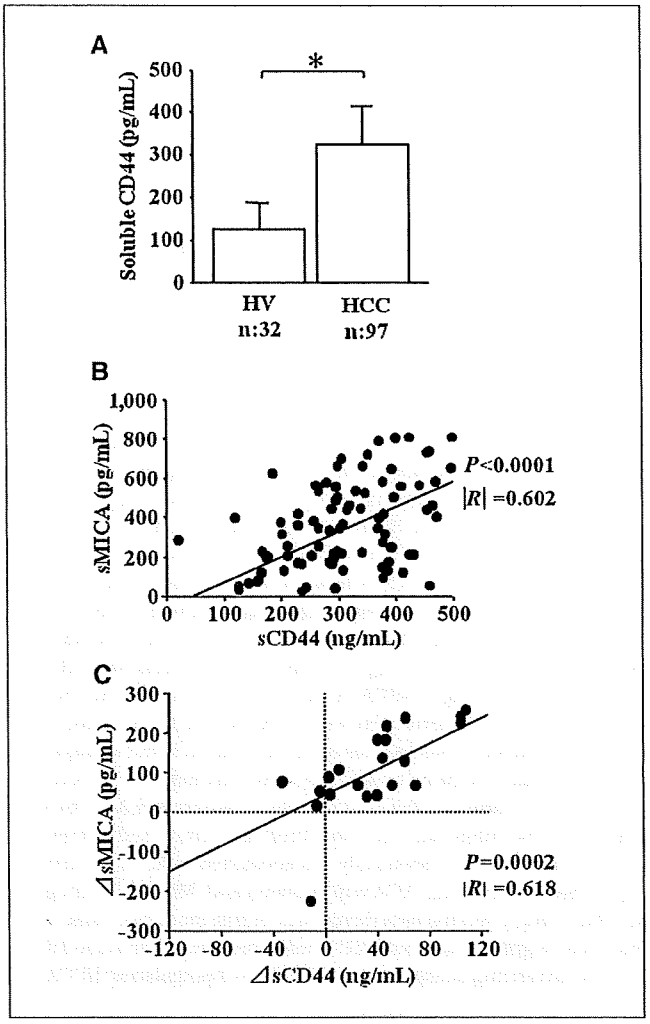

Figure 6. Correlation between soluble CD44 and soluble MICA in human HCC patients. *A* and *B*, soluble CD44 levels and MICA levels in healthy volunteers and HCC patients. Soluble CD44 levels (*sCD44*) and soluble MICA levels (*sMICA*) were determined for sera of HCC patients (n = 97) and age-matched healthy volunteers (*HV*; n = 32). *A*, comparison of sCD44 levels between groups; *B*, correlation between sCD44 levels and sMICA levels in 97 HCC patients. *, P < 0.05. *C*, correlation of sCD44 levels and sMICA levels during TACE therapy. HCC patients (n = 21) treated with epirubicin-based TACE therapy were enrolled and examined for sMICA and sCD44 levels before and 2 wk after therapy. Changes in sMICA (ΔsMICA = serum level of sMICA before TACE treatment − serum level of sMICA after TACE treatment) and those in sCD44 levels (ΔsCD44 = serum level of sCD44 before TACE treatment − serum level of sCD44 after TACE treatment) are plotted.

Discussion

MICA shedding is thought to be a principal mechanism by which tumor cells escape from NKG2D-mediated immunosurveillance (13). Thus, inhibition of MICA shedding should be a reasonable strategy for enhancing antitumor immunity. In the present study, we showed that ADAM10 was overexpressed in human HCC tissues and that ADAM10 knockdown resulted in increased expression of membrane-bound MICA, decreased production of soluble MICA, and upregulation of NK sensitivity of human HCC cells. These results point to ADAM10 as a therapeutic target for inhibiting MICA shedding, thereby ameliorating immunity against HCC. Waldhauer and colleagues recently showed that both ADAM10 and ADAM17 proteases are critically involved in the proteolytic release of soluble MICA of human 293T fibroblast cells and HeLa cervix carcinoma cells (20). Interestingly, in the present study, ADAM17 knockdown failed to affect MICA expression in human HepG2 cells or PLC/PRF/5 cells. Thus, ADAM10, not ADAM17, plays an essential role in the shedding of MICA in human HCC cells. Anderegg and colleagues (23) reported that only ADAM10, not ADAM17, contributed to shedding of CD44 molecules in human melanoma cells although both ADAM10 and ADAM17 proteases were significantly expressed in human melanoma tissues, suggesting that ADAM10 and ADAM17 do not always work in a similar manner. A recent report showed that ADAM10, but not ADAM17, could directly bind to calmodulin (24), which may involve the difference of MICA cleavage between ADAM10 and ADAM17 proteases. Recently, Boutet and colleagues reported that ADAM17 regulates proteolytic shedding of the MICB protein, which is another ligand for the NKG2D receptor on immune cells (25). We previously showed that both soluble MICA and MICB significantly increased in the sera of HCC patients and that therapeutic intervention for HCC leads to reduction of soluble

MICA levels, but not of soluble MICB levels (17), suggesting a more important role of soluble MICA in regulating NKG2D expression after HCC therapy. This led us to focus on the mechanism of MICA shedding in the present study.

Our results revealed that anticancer drugs such as epirubicin and doxorubicin downregulated ADAM10 expression and activity, thereby inhibiting MICA ectodomain shedding. The ADAM family proteins, which are highly expressed in some tumors, play a role in secreting growth factors, such as HB-EGF, and migration of cells. Thus, it is speculated that these proteins could be potential targets for tumor treatment (22). The present study is the first to show that clinically available anticancer drugs have an ability to modulate the expression of ADAM family proteins. They seem to suppress ADAM10 expression at a transcriptional level, but the precise mechanism of this suppression is not yet known.

The MICA ELISA system may not equally detect all soluble MICA (MICA molecules have >60 allelic variants). Our finding that soluble MICA could be detected in all HCC patients suggests that this system was applicable for our cohort of HCC patients. However, special caution should be paid for the use of this ELISA system for widely polymorphic MICA. Because CD44 is well known to be released into circulation from tumors by proteolytic cleavage of ADAM10 (23), the activity of ADAM10 in HCC tissues may be correlated with soluble CD44 levels. If so, our data suggest a close link between ADAM10 activity and the shedding of MICA in HCC. Furthermore, the decline in soluble MICA levels correlated well with the decline in soluble CD44 levels as early as 2 weeks after epirubicin-based TACE therapy. Reducing the tumor volume by such therapy may have led to both decreases but it is also possible that epirubicin suppresses ADAM10 activity, thereby inhibiting the shedding of MICA and CD44. Epirubicin may have a previously unrecognized role in cancer therapy; that is, affecting ADAM10 activity and MICA shedding rather than simply serving as a direct toxic agent for tumor cells.

Our data suggest that anti-HCC chemotherapy could remodel HCC cells, enhancing sensitivity to NK cells by upregulating MICA expression on the cellular surface. A concomitant decline in soluble MICA levels ameliorates NK cell ability by upregulating its NKG2D expression. We previously showed that activation of local innate antitumor immunity in liver tissues resulted in eliciting tumor-specific acquired immunity (21). If liver innate immunity is efficiently activated after anti-HCC chemotherapy, an additional antitumor effect against HCC cells could be expected. Immune modulators such as α-galactosylceramide have been shown to efficiently activate liver innate immune cells, including NK cells (21, 26). The combination therapy of anti-HCC chemotherapy and immunotherapy targeting NK cells might improve the antitumor effect of unresectable HCC and the prognosis of HCC patients.

In spite of recent progress in HCC therapies, there remains significant room for improvement, especially with respect to advanced liver cancer. We have shown here that anti-HCC chemotherapy resulted in enhanced NK sensitivity of HCC cells through inhibition of the activity of ADAM10 protease followed by modification of MICA expression. These findings indicate that efficient activation of liver innate immunity after anti-HCC chemotherapy might represent a particularly promising approach to suppress tumor growth and promote regression in liver cancer patients.

Disclosure of Potential Conflicts of Interest

No potential conflicts of interest were disclosed.

Acknowledgments

Received 3/4/09; revised 7/15/09; accepted 7/24/09; published OnlineFirst 10/13/09.

Grant support: Grant-in-Aid from the Ministry of Education, Culture, Sports, Science and Technology of Japan (T. Takehara) and Grant-in-Aid for Research on Hepatitis and BSE from the Ministry of Health, Labour and Welfare of Japan (N. Hayashi).

The costs of publication of this article were defrayed in part by the payment of page charges. This article must therefore be hereby marked *advertisement* in accordance with 18 U.S.C. Section 1734 solely to indicate this fact.

References

1. Fattovich G, Stroffolini T, Zagni I, Donato F. Hepatocellular carcinoma in cirrhosis: incidence and trends. Gastroenterology 2004;127:S35–50.
2. Bosch FX, Ribes J, Diaz M, Cleries R. Primary liver cancer: worldwide incidence and trends. Gastroenterology 2004;127:S5–16.
3. Takayasu K, Arii S, Ikai I, et al. Prospective cohort study of transarterial chemoembolization for unresectable hepatocellular carcinoma in 8510 patients. Gastroenterol 2006;131:461–9.
4. Doherty DG, O'Farrelly C. Innate and adaptive lymphoid cells in human liver. Immunol Rev 2000;174:5–20.
5. Mehal WZ, Azzaroli F, Crispe IN. Immunology of the healthy liver: old questions and new insights. Gatsroenterology 2001;120:250–60.
6. Bauer S, Groh V, Wu J, et al. Activation of NK cells and T cells by NKG2D, a receptor for stress-inducible MICA. Science 1999;285:727–9.
7. Groh V, Rhinehart R, Seceist H, Bauer S, Grabstein KH, Spies T. Broad tumor-associated expression and recognition by tumor-derived γδT cells of MICA and MICB. Proc Natl Acad Sci U S A 1999;96:6879–84.
8. Jinushi M, Takehara T, Tatsumi T, et al. Expression of MICA and MICB in human hepatocellular carcinomas and their regulation by retinoic acids. Int J Cancer 2003;104:354–61.
9. Wu JD, Higgins LM, Steinle A, Cosman D, Haugk K, Plymate SR. Prevalent expression of the immunostimulatory MHC class I chain-related molecule is counteracted by shedding in prostate cancer. J Clin Invest 2004;114:560–8.
10. Raffaghello L, Prigione I, Airoldi I, et al. Downregulation and/or release of NKG2D ligands as an immune evasion strategy of human neuroblastoma. Neoplasia 2004;6:558–68.
11. Ogasawara K, Lanier LL. NKG2D in NK and T cell-mediated immunity. J Clin Immunol 2005;25:534–40.
12. Coudert JD, Held W. The role of the NKG2D receptor for tumor immunity. Semin Cancer Biol 2006;16:333–43.
13. Groh V, Wu J, Yee C, Spies T. Tumor-derived soluble MIC ligands impair expression of NKG2D and T cell activation. Nature 2002;419:734–8.
14. Salih HR, Rammensee HG, Steinle A. Downregulation of MICA on human tumors by proteolytic shedding. J Immunol 2002;169:4098–102.
15. Salih HR, Antropius H, Gieseke F, et al. Functional expression and release of ligands for activating immunoreceptor NKG2D in leukemia. Blood 2003;102:1389–96.
16. Jinushi M, Takehara T, Tatsumi T, et al. Impairment of natural killer cell and dendritic cell functions by soluble form of MHC class I-related chain A in advanced human hepatocellular carcinoma. J Hepatol 2005;43:1013–20.
17. Kohga K, Takehara T, Tatsumi T, et al. Serum levels of soluble major histocompatibility complex (MHC) class I-related chain A in patients with chronic liver disease and changes during transcatheter arterial embolization for hepatocellular carcinoma. Cancer Sci 2008;99:1643–9.
18. Holdenrieder S, Stieber P, Peterfi A, Nagel D, Steinle A, Salih HR. Soluble MICA in malignant disease. Int J Cancer 2006;118:684–7.
19. Kaiser BK, Yim D, Chow IT, et al. Disulphide-isomerase-enabled shedding of tumor-associated NKG2D ligands. Nature 2007;447:482–6.
20. Waldhauer I, Goehlsdorf D, Gieseke F, et al. Tumor-associated MICA is shed by ADAM proteases. Cancer Res 2008;68:6368–76.
21. Tatsumi T, Takehara T, Yamaguchi S, et al. Intrahepatic delivery of α-galactosylceramide-pulsed dendritic cells suppresses liver tumor. Hepatology 2007;45:22–30.
22. Mochizuki S, Okada Y. ADAMs in cancer cell proliferation and progression. Cancer Sci 2007;98:161–7.
23. Anderegg U, Eichenberg T, Parthaune T, et al. Simon JC. ADAM10 is the constitutive functional sheddase of CD44 in human melanoma cells. J Invest Dermatol 2009;129:1471–82.
24. Nagano O, Murakami D, Hartmann D, et al. Cell-matrix interaction via CD44 is independently regulated by different metalloproteinases activated in response to extracellular domain Ca^{2+} influx and PKC activation. J Cell Biol 2004;165:893–902.
25. Boutet P, Aguera-Gonzalez S, Atkinson S, et al. The metalloproteinase ADAM17/TNF-α enzyme regulates proteolytic shedding of the MHC class I-related chain B protein. J Immunol 2009;182:49–53.
26. Miyagi T, Takehara T, Tatsumi T, et al. CD1d-mediated stimulation of natural killer T cells selectively activates hepatic natural killer cells to eliminate experimentally disseminated hepatoma cells in murine liver. Int J Cancer 2003;106:81–9.

BH3-Only Protein Bid Participates in the Bcl-2 Network in Healthy Liver Cells

Hayato Hikita,[1*] Tetsuo Takehara,[1*] Takahiro Kodama,[1] Satoshi Shimizu,[1] Atsushi Hosui,[1] Takuya Miyagi,[1] Tomohide Tatsumi,[1] Hisashi Ishida,[1] Kazuyoshi Ohkawa,[1] Wei Li,[1] Tatsuya Kanto,[1] Naoki Hiramatsu,[1] Lothar Hennighausen,[2] Xiao-Ming Yin,[3] and Norio Hayashi[1]

Bcl-2 homology domain 3 (BH3)-only protein Bid is posttranslationally cleaved by caspase-8 into its truncated form (tBid) and couples with stress signals to the mitochondrial cell death pathway. However, the physiological relevance of Bid is not clearly understood. Hepatocyte-specific knockout (KO) of Bcl-xL leads to naturally-occurring apoptosis despite co-expression of Mcl-1, which shares a similar anti-apoptotic function. We generated Bcl-xL KO, Bcl-xL/Bid double KO, Bcl-xL/Bak double KO, Bcl-xL/Bax double KO, and Bcl-xL/Bak/Bax triple KO mice and found that hepatocyte apoptosis caused by Bcl-xL deficiency was completely dependent on Bak and Bax, and surprisingly on Bid. This indicated that, in the absence of Bid, Bcl-xL is not required for the integrity of differentiated hepatocytes, suggesting a complicated interaction between core Bcl-2 family proteins and BH3-only proteins even in a physiological setting. Indeed, a small but significant level of tBid was present in wild-type liver under physiological conditions. tBid was capable of binding to Bcl-xL and displacing Bak and Bax from Bcl-xL, leading to release of cytochrome c from wild-type mitochondria. Bcl-xL–deficient mitochondria were more susceptible to tBid-induced cytochrome c release. Finally, administration of ABT-737, a pharmacological inhibitor of Bcl-2/Bcl-xL, caused Bak/Bax-dependent liver injury, but this was clearly ameliorated with a Bid KO background. *Conclusion:* Bid, originally considered to be a sensor for apoptotic stimuli, is constitutively active in healthy liver cells and is involved in the Bak/Bax-dependent mitochondrial cell death pathway. Healthy liver cells are addicted to a single Bcl-2–like molecule because of BH3 stresses, and therefore special caution may be required for the use of the Bcl-2 inhibitor for cancer therapy. (HEPATOLOGY 2009;50:1972-1980.)

Bcl-2 family proteins regulate the mitochondrial pathway of apoptosis in mammalian cells.[1] They are divided into two basic groups: core Bcl-2 family proteins and Bcl-2 homology domain 3 (BH3)-only proteins. Core Bcl-2 family proteins have three or four Bcl-2 homology domains (BH1-BH4 domains), referred to as multidomain members, and structural similarity. These proteins display opposing bioactivities from inhibition to promotion of apoptosis and can be further divided into two groups: anti-apoptotic members, including Bcl-2, Bcl-xL, Bcl-w, Mcl-1, and Bfl-1, and pro-apoptotic members, including Bax and Bak. Pro-apoptotic Bak and Bax are effector molecules of the Bcl-2 family and induce release of cytochrome c from mitochondria, presumably through their ability to form pores at the mitochondrial outer membrane. Anti-apoptotic members, which serve as regulators, inhibit Bak and Bax. The original rheostat model argues for a fine balance between Bax-like pro-apoptotic proteins and Bcl-2–like an-

Abbreviations: ALT, alanine aminotransferase; BH3, Bcl-2 homology domain 3; KO, knockout; tBid, truncated form of Bid; TNF, tumor necrosis factor; TUNEL, terminal deoxynucleotidyl transferase-mediated 2'-deoxyuridine 5'-triphosphate nick-end labeling.

From the [1]Department of Gastroenterology and Hepatology, Osaka University Graduate School of Medicine, Osaka, Japan; [2]Laboratory of Genetics and Physiology, National Institute of Diabetes and Digestive and Kidney Diseases, National Institute of Health, Bethesda, MD; and the [3]Department of Pathology, University of Pittsburgh School of Medicine, Pittsburgh, PA.

**These authors contributed equally to this work and share first authorship.*

Received May 20, 2009; accepted July 21, 2009.

Supported in part by a Grant-in-Aid for Scientific Research from the Ministry of Education, Culture, Sports, Science, and Technology, Japan (to T. Takehara).

Address reprint requests to: Norio Hayashi, M.D., Ph.D., Department of Gastroenterology and Hepatology, Osaka University Graduate School of Medicine, 2-2 Yamada-oka, Suita, Osaka 565-0871, Japan. E-mail: hayashin@gh.med.osaka-u.ac.jp; fax: (81)-6-6879-3629.

Published online in Wiley InterScience (www.interscience.wiley.com).

DOI 10.1002/hep.23207

Potential conflict of interest: Nothing to report.

Additional Supporting Information may be found in the online version of this article.

ti-apoptotic proteins in defining life and death, and this balance would be equal or favor survival in a healthy cell.[2]

BH3-only proteins consist of at least eight members and only share homology with each other and the core Bcl-2 family proteins through the short BH3 motif. They are transcriptionally induced or posttranslationally activated in response to a variety of apoptotic stimuli.[3] When they are induced or activated, they interact with core Bcl-2 family proteins and set the rheostat balance toward apoptosis by directly activating Bax-like molecules or neutralizing Bcl-2–like molecules.[4] Therefore, they serve as initial sensors of apoptotic signals that emanate from various cellular processes. Bid, a member of the BH3-only proteins, is activated via caspase-8–mediated cleavage in response to ligation of the death receptor, and its N-terminal truncated form (tBid) translocates to mitochondria and activates the mitochondrial death pathway.[5] In so-called type 1 cells, such as lymphoid cells, Fas activation leads to caspase-8 activation followed by direct activation of downstream caspases such as caspase-3 and caspase-7, where Bid dose not have significant roles.[6] In contrast, in type 2 cells, Fas-mediated activation of caspase-8 is not enough to activate downstream caspases. In those cells, tBid links the extrinsic or death-receptor pathway to the intrinsic or mitochondrial pathway to execute apoptosis. Hepatocytes are identified as a typical type 2 cell in which Bid plays a critical role in receptor-mediated cell death pathways.[7]

In our previous research, we found that genetic ablation of Bcl-xL in hepatocytes causes spontaneous apoptosis in mice.[8] This indicates that Bcl-xL is a critical apoptosis antagonist in adult healthy hepatocytes, although they possess other anti-apoptotic members of the Bcl-2 family such as Mcl-1. This might be simply explained by the fact that the absence of Bcl-xL affects the rheostat balance of core Bcl-2 family proteins by increasing the ratio of Bax and Bak to anti-apoptotic Bcl-2 proteins. Indeed, neuronal cell death during development caused by Bcl-xL deficiency is ameliorated by loss of Bax.[9] Platelet cell death caused by Bcl-xL deficiency is also ameliorated by loss of Bak.[10] These studies indicate that the stoichiometry between Bcl-xL and Bax or Bak dictates cellular fate. However, the possibility of BH3-only proteins being involved in the apoptosis rheostat in healthy cells has not been addressed. We generated Bcl-xL/Bid double-knockout (KO) mice and demonstrated that apoptosis caused by Bcl-xL deficiency is critically dependent on Bid. A small amount of Bid appears to be activated in the liver under physiological conditions and to be significant for inducing cytochrome c release from Bcl-xL–deficient mitochondria. This study shed light on the active participation of BH3-only proteins, which are generally considered to be sensors of apoptotic stimuli, in the Bcl-2 network regulating life and death of healthy differentiated hepatocytes.

Materials and Methods

Mice. Mice carrying a *bcl-x* gene with 2 *lox*P sequencers at the promoter region and a second intron ($bcl\text{-}x^{flox/flox}$) were described previously.[11] Heterozygous AlbCre transgenic mice expressing Cre recombinase gene under the promoter of the albumin gene[8] and traditional Bid KO mice[7] also have been described previously. We purchased from the Jackson Laboratory (Bar Harbor, ME) traditional Bak KO mice, traditional Bax KO mice, and conditional Bak/Bax KO mice ($bak^{-/-}$ $bax^{flox/flox}$).[12] We generated hepatocyte-specific Bcl-xL KO mice ($bcl\text{-}x^{flox/flox}$ *AlbCre*), Bcl-xL/Bid double-KO mice ($bid^{-/-}$ $bcl\text{-}x^{flox/flox}$ *AlbCre*), Bcl-xL/Bak double-KO mice ($bak^{-/-}$ $bcl\text{-}x^{flox/flox}$ *AlbCre*), Bcl-xL/Bax double-KO mice ($bax^{-/-}$ $bcl\text{-}x^{flox/flox}$ *AlbCre*), and Bcl-xL/Bak/Bax triple-KO mice ($bak^{-/-}$ $bax^{flox/flox}$ $bcl\text{-}x^{flox/flox}$ *AlbCre*) by mating the strains. They were maintained in a specific pathogen-free facility and treated with humane care under approval from the Animal Care and Use Committee of Osaka University Medical School.

Apoptosis Assay. The levels of serum alanine aminotransferase (ALT) were measured by a standard method, and serum caspase-3/7 activity was measured by a luminescent substrate assay for caspase-3 and caspase-7 (Caspase-Glo assay, Promega, Tokyo, Japan). The caspase-3/7 activity was normalized by each control group. For histological analysis, the liver sections were stained with hematoxylin-eosin. To detect cells with oligonucleosomal DNA breaks, the sections were also subjected to terminal deoxynucleotidyl transferase-mediated deoxyuridine triphosphate nick-end labeling (TUNEL) staining, according to a previously reported procedure.[13]

Western Blot Analysis. Liver tissue was lysed with a lysis buffer (1% Nonidet P-40, 0.5% sodium deoxycholate, 0.1% sodium dodecyl sulfate, 1 × protein inhibitor cocktail (Nacalai tesque, Kyoto, Japan), phosphate-buffered saline, pH 7.4). Equal amounts of protein were electrophoretically separated by sodium dodecyl sulfate polyacrylamide gels and transferred onto polyvinylidene fluoride membrane. For immunodetection, the following antibodies were used: anti-Bcl-xL antibody (Santa Cruz Biotechnology, Santa Cruz, CA), anti-Mcl-1 antibody (Rockland, Gilbertsville, PA), previously described anti-Bid antibody generated from glutation-S-transferase-Bid fusion protein,[14] anti-full-length Bid antibody, anti-cleaved caspase-7 antibody, anti-Bax antibody, anti-Cox IV antibody (Cell Signaling Technology, Beverly, MA),

anti-Bak antibody (Millipore, Billerica, MA), and anti–β-actin antibody (Sigma-Aldrich, St. Louis, MO).

Isolation of Mitochondria-Rich and Cytosolic Fraction. After liver tissue was homogenized using isolation buffer (225 mM mannitol, 75 mM sucrose, 0.1 mM ethylene glycol tetraacetic acid, 1 mg/mL fatty acid–free bovine serum albumin, 1 × protein inhibitor cocktail, 10 mM 4-(2-hydroxyethyl)-1-piperazine ethanesulfonic acid–potassium hydroxide, pH 7.4), the lysate was centrifuged at 600*g* for 10 minutes, and the supernatant was centrifuged at 15,000*g* for 10 minutes. The pellet was regarded as a mitochondria-rich fraction and the supernatant as a cytosolic fraction.

Immunoprecipitation of Bcl-xL. Approximately 30 mg liver tissue was lysed with a TNE buffer (1% Nonidet P-40, 1 mM ethylenediaminetetra-acetic acid, 1 × protein inhibitor cocktail, 0.15 M NaCl, 10 mM Tris-HCl, pH 7.8). Equal amounts of protein samples were rotated with protein G sepharose (GE Healthcare, Tokyo, Japan) and anti-Bcl-xL antibody (Abcam, Cambridge, MA) overnight at 4°C. After centrifugation, the pellet was collected as the immunoprecipitate protein.

Incubation of tBid or Bid for Immunoprecipitation. Liver tissue (90 mg) was lysed with 800 μL lysis buffer (2 mM ethylenediaminetetra-acetic acid, 10 mM ethylene glycol tetra-acetic acid, 50 mM NaF, 5 mM $Na_2P_4O_7$, 10 mM β-glycerophosphate, 0.1% 2-mercaptoethanol, 1% Triton X, 1 × protein inhibitor cocktail, 50 mM Tris-HCl, pH 7.5). Equal volumes of protein samples were incubated with or without recombinant mouse tBid or full-length Bid (R&D Systems, Minneapolis, MN).

Analysis of Cytochrome C Release. The mitochondria-rich fraction was diluted in a mitochondria dilution buffer (395 mM sucrose, 0.1 mM ethylene glycol tetra-acetic acid, 10 mM 4-(2-hydroxyethyl)-1-piperazine ethanesulfonic acid–potassium hydroxide, pH 7.4). The diluted mitochondria were incubated with recombinant mouse tBid or full-length Bid diluted with a reaction buffer (125 mM KCl, 0.5 mM $MgCl_2$, 3.0 mM succinic acid, 3.0 mM glutamic acid, 10 mM 4-(2-hydroxyethyl)-1-piperazine ethanesulfonic acid–potassium hydroxide, 1 × protein inhibitor cocktail, 2.5 mM ethylenediaminetetra-acetic acid and BOC-Asp (OMe) CH_2F 20 μM, pH 7.4) for 30 minutes at 37°C. The levels of cytochrome c in the buffer were determined using an enzyme-linked immunosorbent assay kit (R&D Systems). The maximum or spontaneous release of cytochrome c was defined as the level of samples incubated with 0.1% Triton X-100 or medium alone, respectively. The percentage release of cytochrome c was calculated using the following formula:

% release = (experimental release − spontaneous release) × 100/(maximum release − spontaneous release).

ABT-737 Injection Study. ABT-737 was provided by Abbott Laboratories (Abbott, Park, IL). ABT-737 was dissolved with a mixture of 30% propylene glycol, 5% Tween 80, and 65% D5W (5% dextrose in water), final pH 4 to 5. Mice were given a single intraperitoneal injection of ABT-737 at 100 mg/kg and sacrificed 16 hours later. Platelets were counted using an automated cell counter (Sysmex, Kobe, Japan).

Statistical Analysis. Data are presented as mean ± standard deviation. Multiple comparisons of TUNEL-positive cells were performed by analysis of variance followed by Fisher's *post hoc* correction. The other multiple comparisons were performed by analysis of variance followed by Scheffe *post hoc* correction. $P < 0.05$ was considered statistically significant.

Results

Hepatocyte Apoptosis Caused by Bcl-xL Deficiency Is Completely Lost with Bid-Deficient Background. To examine the possibility of whether Bid is involved in apoptosis caused by Bcl-xL deficiency, hepatocyte-specific Bcl-xL KO mice were crossed with traditional Bid KO mice. After mating *bid*$^{+/-}$ *bcl-x*$^{flox/flox}$ *AlbCre* mice with *bid*$^{+/-}$ *bcl-x*$^{flox/flox}$ mice, western blot analysis confirmed lack of Bcl-xL and Bid in the liver of Bcl-xL KO mice and Bid KO mice, respectively, and intermediate expression of Bid in the Bid+/- liver (Fig. 1A). Consistent with our previous findings,[8] Bcl-xL KO mice (*bid*$^{+/+}$ *bcl-x*$^{flox/flox}$ *AlbCre*) produced spontaneous hepatocyte apoptosis (Fig. 1B), which was associated with caspase-7 activation in the liver (Fig. 1C). Serum ALT levels (Fig. 1D), caspase-3/7 activity (Fig. 1E), and the frequency of TUNEL-positive hepatocytes (Fig. 1F) were significantly higher in Bcl-xL KO mice than in wild-type mice (*bid*$^{+/+}$ *bcl-x*$^{flox/flox}$). Bid KO mice (*bid*$^{-/-}$ *bcl-x*$^{flox/flox}$) did not produce any liver phenotypes under physiological conditions, in agreement with a previous report.[7] This was further confirmed by our additional analysis on Bid KO mice and control littermates, which showed no difference in serum ALT levels (Supporting Fig. 1A), caspase-3/7 activity (Supporting Fig. 1B), and the ratios of liver weight to body weight (Supporting Fig. 1C). Of importance is the finding that serum ALT levels were reduced to the normal levels in Bcl-xL/Bid double-KO mice (*bid*$^{-/-}$ *bcl-x*$^{flox/flox}$ *AlbCre*). Bcl-xL KO with Bid heterozygosity (*bid*$^{+/-}$ *bcl-x*$^{flox/flox}$ *AlbCre*) displayed intermediate ALT levels between Bcl-xL KO mice and double-KO mice. In agreement with this observation, the number of TUNEL-positive hepatocytes in Bcl-xL/Bid double-KO mice reached background levels. In addition, the levels of caspase-3/7 activity in serum were also normalized in Bcl-xL/Bid double-KO mice. Taken together, these observations indicated that

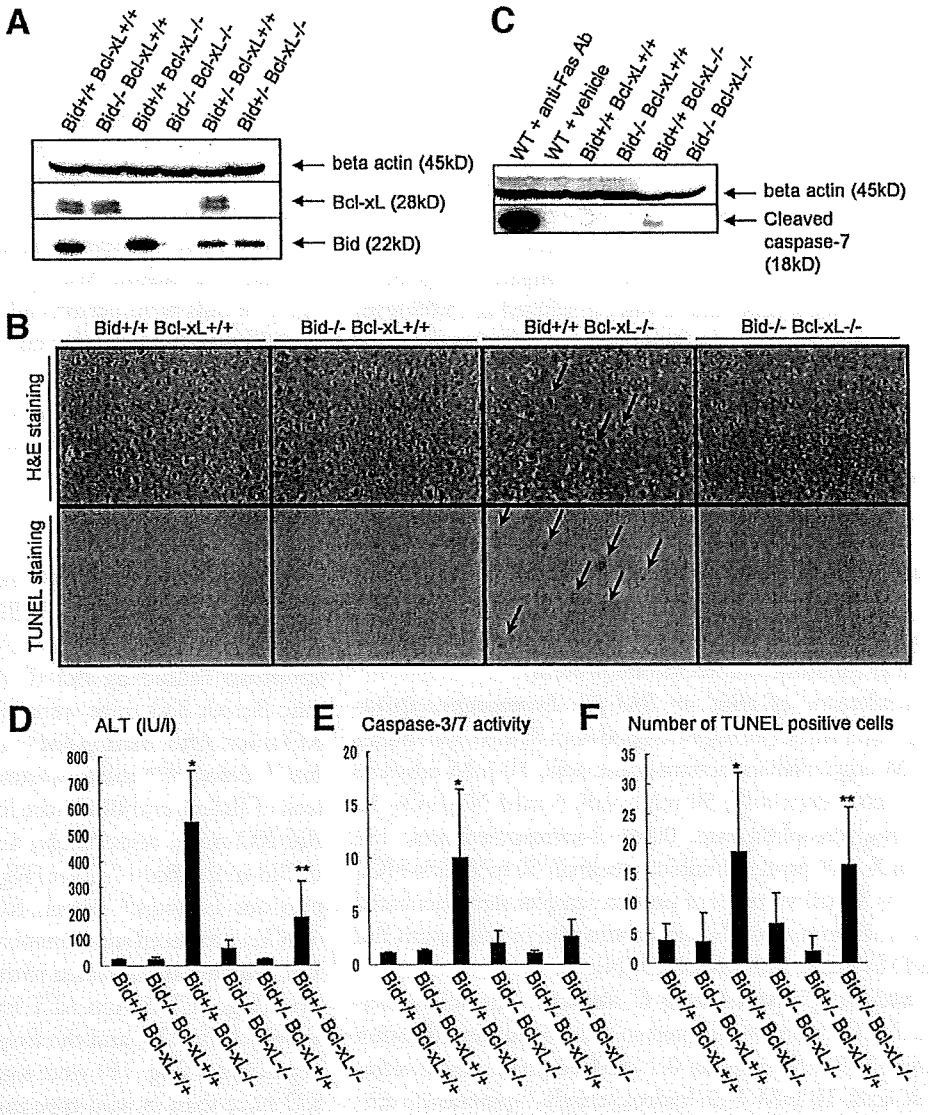

Fig. 1. Bcl-xL/Bid double-KO mice. Offspring from mating *bid*$^{+/-}$ *bcl-x*$^{flox/flox}$ *AlbCre* mice and *bid*$^{+/-}$ *bcl-x*$^{flox/flox}$ mice were sacrificed at 6 weeks after birth. Bcl-xL+/+ stands for *bcl-x*$^{flox/flox}$ without *AlbCre*, and Bcl-xL−/− stands for *bcl-x*$^{flox/flox}$ with *AlbCre*. (A) Western blot of whole liver lysate for the expression of Bcl-xL and Bid. (B) Representative pictures of liver histology stained with hematoxylin-eosin and TUNEL. Arrows indicate typical apoptotic cells. (C) Western blot of whole liver lysate for the expression of cleaved caspase-7. Live lysates from wild-type mice 3 hours after intraperitoneal injection of 30 μg anti-Fas antibody (clone Jo2) or vehicle were included as a positive and a negative control, respectively. (D) Serum ALT levels. N = 14 mice per group. *$P < 0.05$ versus the other five groups; **$P < 0.05$ versus the other four groups except Bid−/− Bcl-xL−/− group. (E) Serum caspase-3/7 activity. N = 13 mice per group. *$P < 0.05$ versus the other five groups. (F) Statistics of TUNEL- positive cells. N = 6 mice per group. * and **$P < 0.05$ versus all of Bcl-xL +/+ groups and Bid−/− Bcl-xL−/− group.

apoptosis caused by Bcl-xL deficiency is completely dependent on the BH3-only protein Bid. Bid is activated by tumor necrosis factor (TNF) receptor,[15] and TNF-α, which is a ligand of TNF receptor, is produced by Myd88 signal pathway.[16] To examine the possibility of involvement of Myd88 or TNF-α in this apoptosis, we generated Myd88 Bcl-xL double-KO mice by crossing myd88$^{-/-}$ mice with bcl-x$^{flox/flox}$ AlbCre mice and administered neutralizing anti–TNF-α antibody into Bcl-xL KO mice. Hepatocyte apoptosis caused by Bcl-xL deficiency was not ameliorated with Myd88 KO background or by administration of anti–TNF-α antibody (Supporting Fig. 2A, B).

Hepatocyte Apoptosis Caused by Bcl-xL Deficiency Requires Both Bak and Bax. To depict the precise relationships among core Bcl-2 family proteins in regulating liver homeostasis, hepatocyte-specific Bcl-xL–deficient mice were crossed with traditional Bak or Bax KO mice. The levels of serum ALT were slightly decreased with a Bak KO background (*bak*$^{-/-}$ *bcl-x*$^{flox/flox}$ *AlbCre*), whereas they did not change with a Bax KO background (*bax*$^{-/-}$ *bcl-x*$^{flox/flox}$ *AlbCre*) (Fig. 2A, B). To examine the contribution of both Bax and Bak, Bcl-xL KO mice were crossed with conditional Bak/Bax KO mice. The levels of serum ALT were completely normalized in Bak/Bax KO background (*bak*$^{-/-}$ *bax*$^{flox/flox}$ *bcl-x*$^{flox/flox}$ *AlbCre*) (Fig. 2C). Hepatocyte apoptosis determined by TUNEL staining of liver sections and caspase activation determined by caspase-3/7 activity in serum also returned to background levels (Fig. 2D, E). These observations clearly indicated that apoptosis caused by Bcl-xL deficiency was generated through the Bak/Bax-dependent mitochondrial cell death pathway. To clarify the background levels of hepatocyte apoptosis, we also analyzed the liver apoptosis in *bak*$^{-/-}$ and *bak*$^{-/-}$ *bax*$^{flox/flox}$ *AlbCre* mice. Similarly, in *bid*$^{-/-}$

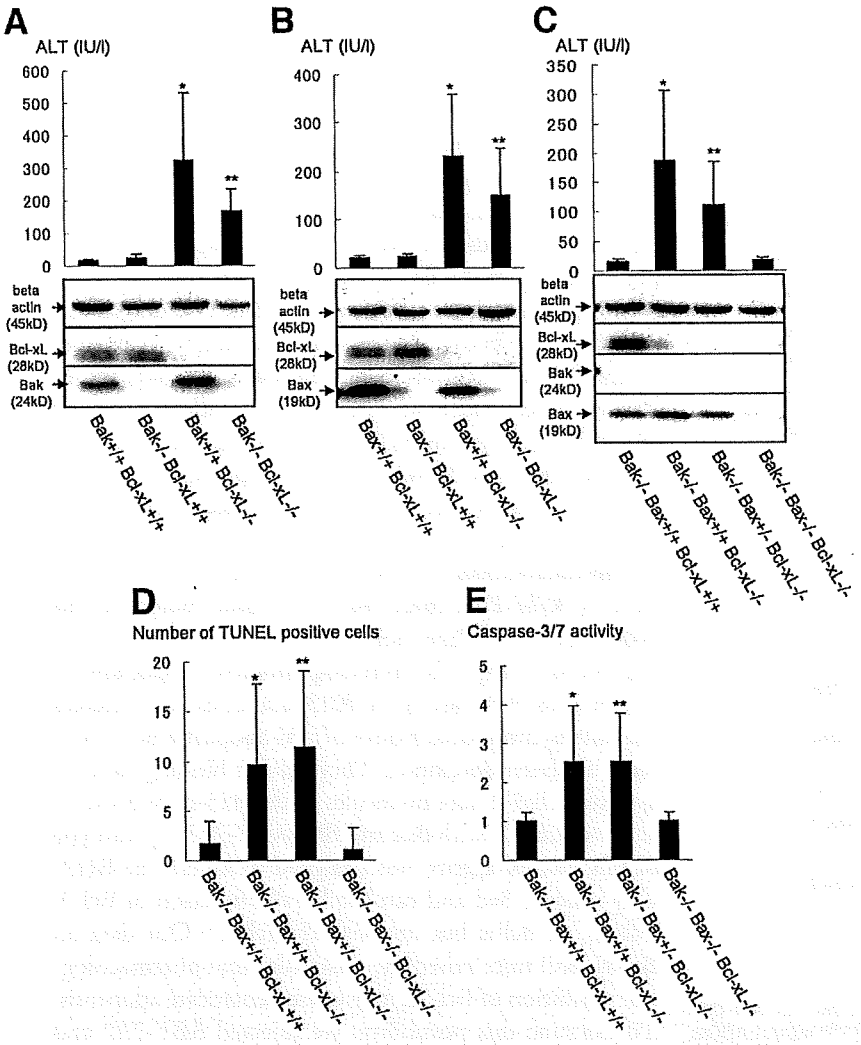

Fig. 2. Bcl-xL KO mice with Bak or Bax KO background. (A) Offspring from mating *bak*$^{+/-}$ *bcl-x*$^{flox/flox}$ *AlbCre* mice and *bak*$^{+/-}$ *bcl-x*$^{flox/flox}$ mice were sacrificed at 6 weeks after birth. Serum ALT levels and western blot of whole liver lysate for the expression of Bcl-xL and Bak are shown. N = 14 mice per group. * and **$P < 0.05$ versus the other three groups. (B) Offspring from mating *bax*$^{+/-}$ *bcl-x*$^{flox/flox}$ *AlbCre* mice and *bax*$^{+/-}$ *bcl-x*$^{flox/flox}$ mice were sacrificed at 6 weeks after birth. Serum ALT levels and western blot of whole liver lysate for the expression of Bcl-xL and Bax are shown. N = 15 mice per group. * and **$P < 0.05$ versus the other two Bcl-xL+/+ groups. (C, D, and E) Offspring from mating *bak*$^{-/-}$ *bax*$^{flox/+}$ *bcl-x*$^{flox/flox}$ *AlbCre* mice and *bak*$^{-/-}$ *bax*$^{flox/+}$ *bcl-x*$^{flox/flox}$ mice were sacrificed at 6 weeks after birth. Bax+/+ stands for *bax*$^{flox/flox}$ without *AlbCre*, and Bax−/− stands for *bax*$^{flox/flox}$ with *AlbCre*. N = 8 or 10 mice per group. Serum ALT levels and western blot of whole liver lysate for the expression of Bcl-xL, Bak, and Bax are shown (C). *$P < 0.05$ versus Bak−/− Bax+/+ Bcl-xL+/+ and Bak−/− Bax−/− Bcl-xL−/− groups; **$P < 0.05$ versus Bak−/− Bax−/− Bcl-xL−/− group. Statistics of TUNEL-positive cells (D). * and **$P < 0.05$ versus Bak−/− Bax+/+ Bcl-xL+/+ and Bak−/− Bax−/− Bcl-xL−/− groups. Serum caspase-3/7 activity (E). * and **$P < 0.05$ versus Bak−/− Bax+/+ Bcl-xL+/+ and Bak−/− Bax−/− Bcl-xL−/− groups.

mice, there was no difference between two groups in serum ALT levels (Supporting Fig. 3A), caspase-3/7 activity (Supporting Fig. 3B), and the ratios of liver weight to body weight (Supporting Fig. 3C), which suggests that healthy hepatocytes in wild-type mice are completely protected from Bid or Bak/Bax-mediated apoptosis by Bcl-xL.

Bcl-xL Interacts with Cytosolic Bax and Mitochondrial Bak in the Liver. To examine the expression of a variety of Bcl-2–related molecules in the liver, cytosolic and mitochondrial fractions from liver lysate were subjected to western blot analysis (Fig. 3A). Anti-apoptotic Bcl-2 proteins, Bcl-xL and Mcl-1, were expressed at both the mitochondria and the cytosol. In contrast, Bak and Bax were exclusively expressed at the mitochondria and the cytosol, respectively. Full-length Bid was expressed mainly in the cytosol. To examine whether Bcl-xL physically interacts with those Bcl-2–related proteins, liver lysate was immunoprecipitated with Bcl-xL and identified using corresponding antibodies (Fig. 3B). At least a part of Bcl-xL was bound to Bak and Bax, but not to Mcl-1 or full-length Bid.

tBid, But Not Full-Length Bid, Displaces Bak and Bax from Bcl-xL by Binding to Bcl-xL. Bcl-2–like molecules have been shown to be capable of binding Bak or Bax, and through this interaction, to neutralize each activity.[17] Conversely, other research showed that Bcl-xL does not have to bind Bax-like molecules to protect against cell death.[18] To examine the impact of tBid on the association between Bcl-xL and Bak or Bax, we added tBid to the liver lysate and examined the interaction of each Bcl-2–related protein with Bcl-xL by immunoprecipitation. Addition of 500 nM tBid abolished the association between Bcl-xL and Bak or Bax (Supporting Fig. 4). Simultaneously, Bcl-xL binding of tBid was observed. Addition of 20 nM tBid also abolished, if not completely, the association between Bcl-xL and Bak or Bax (Fig. 4). In contrast, adding the same concentration of full-length Bid had little effect on Bcl-xL binding of Bak or Bax (Fig. 4). These results indicated that tBid can bind to Bcl-xL

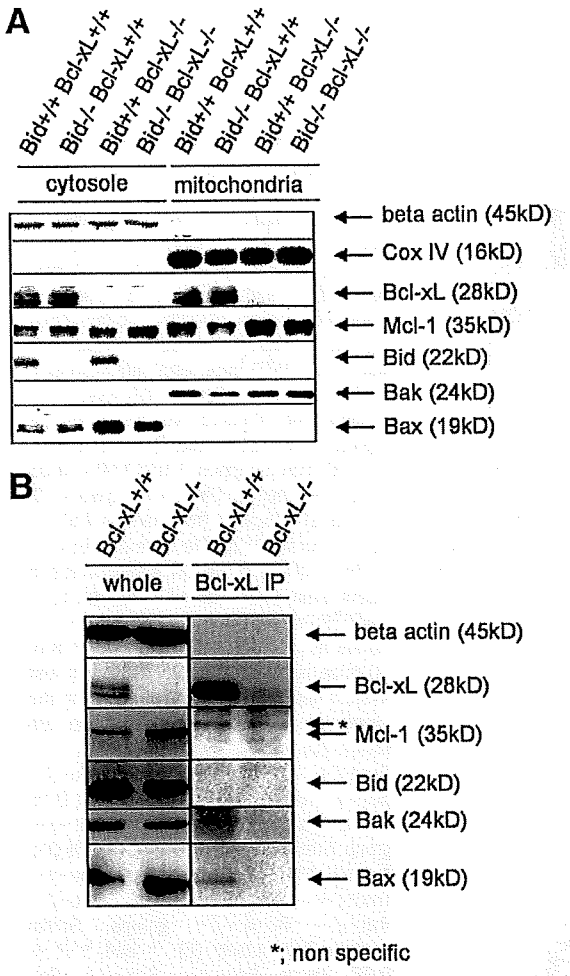

Fig. 3. Expression of Bcl-2-related molecules in the liver and their association with Bcl-xL. Bcl-xL+/+ stands for *bcl-x*$^{flox/flox}$ without *AlbCre*, and Bcl-xL−/− stands for *bcl-x*$^{flox/flox}$ with *AlbCre*. (A) Western blot after cellular fractionations of the liver lysate. Loading amounts of cytosolic and mitochondrial fractions were adjusted to be equivalent for the starting liver samples. (B) Western blot after anti-Bcl-xL immunoprecipitation. Whole cellular lysate and immunoprecipitates with anti-Bcl-xL were verified with the indicated antibodies. Samples from Bcl-xL−/− mice were included as a negative control.

and suggest that tBid binding of Bcl-xL unleashes Bak or Bax from Bcl-xL.

A Small But Significant Level of tBid Is Detected in the Healthy Liver. Genetic evidence that Bid is required for Bak/Bax-dependent apoptosis caused by Bcl-xL deficiency and biochemical evidence that full-length Bid is inactive for displacing Bak or Bax from Bcl-xL together suggest that tBid is produced in wild-type liver. To confirm this, we performed western blot analysis using antibody that can detect tBid (Fig. 5A). Liver lysate from Bid KO mice served as a negative control, whereas that from wild-type mice injected with anti-Fas antibody served as a positive control. A significant level of tBid was detected in wild-type liver, although the amount was smaller than in Fas-stimulated mice, which displayed massive live cell apoptosis.

Bcl-xL–Deficient Mitochondria Are Susceptible to a Trace Amount of tBid. To examine the impact of a small amount of tBid on Bcl-xL–deficient mitochondria, tBid or full-length Bid at various concentrations was incubated with mitochondria isolated from Bcl-xL–deficient liver or wild-type liver (Fig. 5B). In agreement with previous reports,[19] wild-type mitochondria efficiently released cytochrome c on exposure to tBid. Full-length Bid was far less effective at releasing cytochrome c. Importantly, Bcl-xL–deficient mitochondria were capable of releasing cytochrome c on exposure to a smaller amount of tBid than wild-type mitochondria. This agrees with the in vivo findings that Bcl-xL–deficient hepatocytes, but not wild-type hepatocytes, underwent apoptosis with a trace amount of tBid.

Administration of ABT-737 Produces ALT Elevation in Wild-Type Mice But to a Lesser Extent in Bid KO Mice. Bcl-2–like molecules have been receiving attention as a target for inducing apoptosis, especially in cancer cells.[20] A variety of BH3 mimetics that interact with the hydrophobic groove of anti-apoptotic Bcl-2 proteins has been developed. They inhibit binding of anti-apoptotic Bcl-2–like molecules with BH3-only proteins and presumably with Bak and Bax. ABT-737, a prototype of this class of agents, was designed to mimic the BH3-only protein Bad and can inhibit the function of Bcl-2, Bcl-xL, or Bcl-w but not that of Mcl-1.[21] Our data on Bcl-xL KO mice raised the possibility that pharmacological inhibition of Bcl-xL may cause hepatocyte apoptosis. To examine this possibility, we injected ABT-737 and examined the liver injury. As expected, the levels of ALT

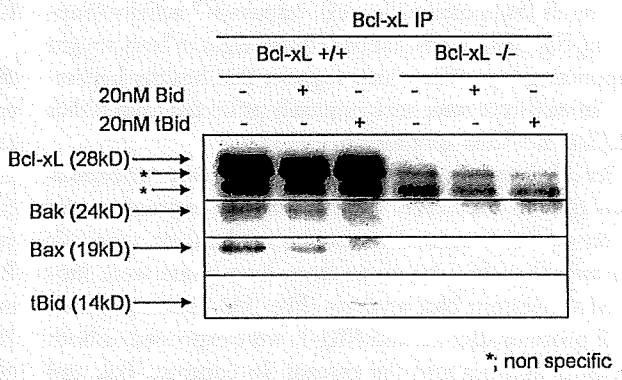

Fig. 4. tBid binds to Bcl-xL and displaces Bak or Bax from Bcl-xL. Liver lysate from *bcl-x*$^{flox/flox}$ without *AlbCre* (Bcl-xL+/+) and *bcl-x*$^{flox/flox}$ with *AlbCre* (Bcl-xL−/−) were incubated with or without 20 nM recombinant tBid or recombinant full-length Bid at 37°C for 20 minutes. After immunoprecipitation with Bcl-xL, immunoprecipitates are verified with indicated antibodies. Immunoprecipitated lysate from Bcl-xL−/− mice was loaded as a negative control.

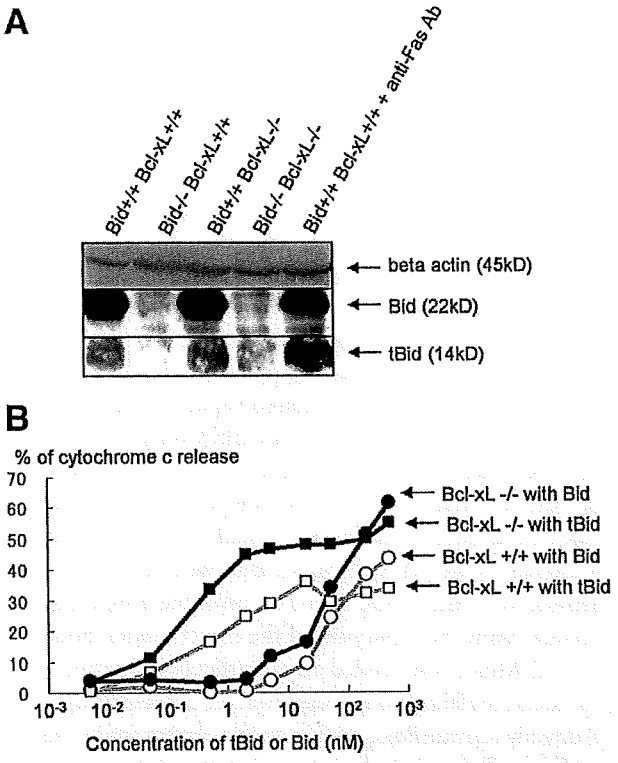

Fig. 5. A small amount of tBid is expressed in wild-type liver and is sufficient for producing cytochrome c release from Bcl-xL–deficient mitochondria. (A) Western blot of liver lysate for Bid and tBid expression. Lysate from wild-type (Bid+/+ Bcl-xL+/+) mice 1 hour after intravenous injection of 10 μg anti-Fas antibody (clone Jo2) and from Bid−/− mice were included as a positive and a negative control of tBid, respectively. (B) Mitochondrial release of cytochrome c to tBid. Mitochondria were isolated from Bcl-xL–deficient or wild-type liver and incubated with recombinant tBid or recombinant full-length Bid at various concentrations for 30 minutes. Similar results were obtained in three times repeated experiments.

were clearly elevated in wild-type mice (Fig. 6A). TUNEL staining of the liver section showed apoptosis in hepatocytes scattered in the liver lobule (Fig. 6B). Importantly, no significant elevation of serum ALT levels was observed with a Bak/Bax double-KO background. The data indicated that genetic and pharmacological ablation of Bcl-xL led to a similar apoptosis phenotype in the liver.

To examine the impact of Bid in ABT-737–induced hepatocyte apoptosis, ABT-737 was administered to wild-type mice and Bid KO mice. Elevation of serum ALT levels was ameliorated with a Bid KO background (Fig. 6C). It has been well established that administration of ABT-737 led to acute thrombocytopenia.[22] This was explained by the fact that Bcl-xL is a critical apoptosis antagonist in platelets.[10] In our experiment, the counts of circulating platelets declined significantly in the wild-type mice (Fig. 6D), which is in the agreement with previous studies.[10] Interestingly, a similar degree of thrombocytopenia was observed even in Bid KO mice, suggesting that Bid does not play a significant role in regulating platelet homeostasis, unlike in hepatocytes. The data imply that the impact of Bid in the Bcl-2 network in healthy cells is cell-type specific.

Discussion

One of the important findings of the current study is that the BH3-only protein Bid is an essential molecule for apoptosis of differentiated hepatocytes caused by Bcl-xL deficiency. This is surprising, because differentiated hepatocytes are generally considered to be quiescent cells. Organ homeostasis may be ensured in two ways: one is through turnover of cells, and the other is by the quies-

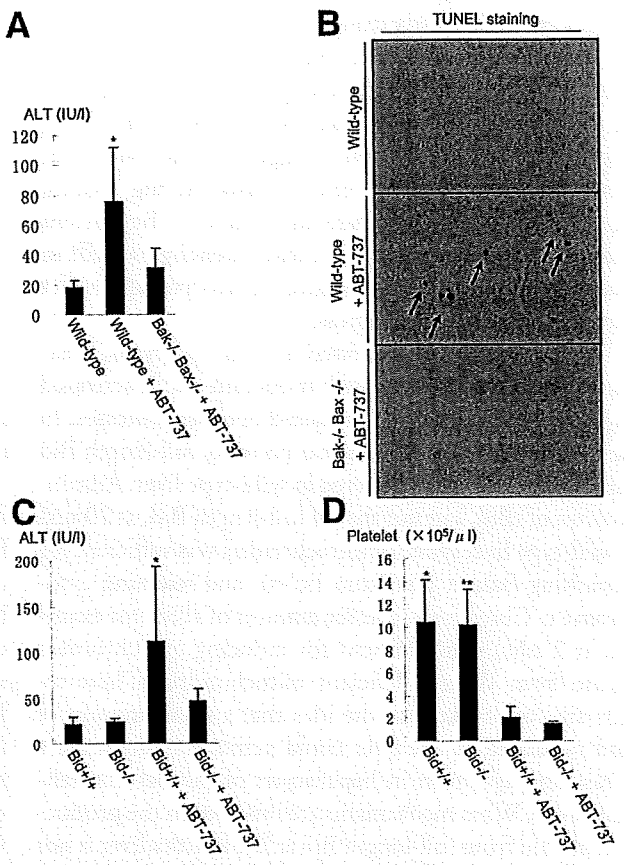

Fig. 6. ABT-737 administration in wild-type, Bak/Bax double-KO, and Bid KO mice. (A and B) Wild-type mice or hepatocyte-specific Bak/Bax double-KO mice were challenged with intraperitoneal injection of ABT-737 at 100 mg/kg or vehicle alone and sacrificed 16 hours later. Serum ALT levels (A) and representative pictures of TUNEL staining in the liver (B) are shown. N = 5 or more than 5 mice per group. *$P < 0.05$ versus the other two groups. (C and D) Wild-type mice or Bid KO mice were challenged with intraperitoneal injection of ABT-737 at 100 mg/kg or vehicle alone and sacrificed 16 hours later. Serum ALT levels (C) and circulating platelet counts (D) were determined. N = 5 or more than 5 mice per group. *$P < 0.05$ versus the other three groups for (C); * and **$P < 0.05$ versus the other two groups, with ABT-737 for (D).

cence of matured cells. Typical examples for the former are hematopoietic organs, intestine and skin, whereas those for the latter are a variety of solid organs, such as the liver, lung, pancreas, heart, and brain. Because hematopoietic cells die at particular time points to maintain host homeostasis, it would not be surprising that their life span may be controlled by a variety of death signals. Indeed, Bim KO mice have excess hematopoietic cells, particularly lymphocytes, suggesting that Bim strictly controls homeostasis of hematopoietic cells.[23] In contrast, healthy cells in the solid organs are usually considered to not suffer from apoptotic stimuli. Although interaction between core Bcl-2 proteins and BH3-only proteins is important for understanding apoptosis regulation, little work has been done by generating mice simultaneously deficient in molecules of both groups. To the best of our knowledge, the only example clearly using this approach is a study on Bim/Bcl-2 double-KO mice that showed that growth retardation, skin abnormality, and lymphoid cell reduction found in Bcl-2 KO mice were ameliorated with a Bim-deficient background.[24] This suggested that lymphoid cells constitutively sense Bim-mediated killing signals, and, without Bcl-2, decrease in number. The current study is the first demonstration that parenchymal cells in a solid organ such as differentiated hepatocytes also suffer from Bid-mediated BH3 stress.

Bid is ubiquitously expressed in many cell types. Generally, Bid is inactive for death induction and is activated on proteolytic cleavage by caspase-8 or other proteases. In the current study, we found that not only full-length Bid but also tBid could be detected in wild-type liver. Administration of tBid, but not that of full-length Bid, at 20 nM in wild-type liver lysate or mitochondria was sufficient for unleashing Bak or Bax from Bcl-xL and releasing cytochrome c. Conversely, a lesser amount of tBid (for example, at 2 nM) was sufficient for inducing cytochrome c release from Bcl-xL–deficient mitochondria. These results are consistent with the idea that a small amount of tBid produced in the liver could activate cytochrome c release and apoptosis in hepatocytes of the Bcl-xL–deficient mice. What mechanisms are involved in the production of tBid from full-length Bid in the healthy liver is not known yet. Our results suggest that Myd88 and TNF-α may not be involved in the activation of tBid under physiological conditions. However, other ligation of death receptors such as Fas, and TNF-related apoptosis-inducing ligand receptor, can cause caspase-8 activation followed by Bid cleavage.[15,25] Bile salts, which are consistently produced in and secreted from hepatocytes, are capable of inducing hepatocyte apoptosis through Fas activation.[26] Natural killer cells are predominant lymphocytes accumulating in the liver and constitutively express TNF-related apoptosis-inducing ligand.[27] Further study is needed to examine what kinds of stresses activate the Bid pathway in a physiological setting.

Adult differentiated hepatocytes express at least two anti-apoptotic Bcl-2 proteins, Bcl-xL and Mcl-1, but not prototype Bcl-2.[8] Recently, Vick et al.[28] reported that hepatocyte-specific Mcl-1 KO mice developed naturally occurring apoptosis in hepatocytes. We also independently generated hepatocyte-specific Mcl-1 KO mice and obtained an apoptosis phenotype that could not be distinguished from that of hepatocyte-specific Bcl-xL KO mice.[29] Thus, Mcl-1, like Bcl-xL, plays a critical role in maintaining integrity of differentiated hepatocytes. There are two major models regarding how BH3-only proteins mediate Bak/Bax-dependent apoptosis: a direct model and an indirect model.[30] From the viewpoint of the indirect model, our data would mean a small amount of tBid is sequestered by Bcl-xL and Mcl-1 and, without Bcl-xL, is sufficient for neutralizing Mcl-1 to promote apoptosis. Conversely, from the viewpoint of the direct model, both Bcl-xL and Mcl-1 are needed to completely sequester a small amount of tBid, and without Bcl-xL, unleashed tBid would directly activate Bak and Bax. In the current study, we observed that tBid when administered in liver lysate could bind to Bcl-xL. This observation seems to agree with the indirect model, although we could not exclude the possibility of the direct model. Further study will be needed by developing Bid/Bcl-xL/Mcl-1 KO mice to examine the underlying mechanisms of how activated Bid regulates the mitochondrial pathway of apoptosis in the liver.

Malignant tumors frequently overexpress one or more members of the anti-apoptotic Bcl-2 family, which confers the resistance of tumor cells to apoptosis.[31,32] Recently, small molecules targeting specific anti-apoptotic Bcl-2 family proteins have been developed for treatment of cancer therapy.[33,34] The underlying concept of this strategy is the difference in addiction to anti-apoptotic Bcl-2 family proteins between normal cells and transformed cells. In general, normal cells are not considered to suffer from apoptotic stimuli or to have activated BH3-only proteins. In contrast, transformed cells suffer from a variety of apoptotic stimuli such as genotoxic *p53* activation and environmental stresses, and possess activated BH3-only molecules. If a single anti-apoptotic Bcl-2 protein is neutralized by a small molecule, it could release BH3-only molecules, which then neutralize other anti-apoptotic Bcl-2 proteins or directly activate Bax-like molecules, leading to cell death. However, the current study clearly indicated that normal hepatocytes could be under activation of Bid, raising concern that hepatocyte injury may be produced if Bcl-xL function is completely knocked down. Indeed, we have shown that administra-

tion of a high dose of ABT-737, which is an antagonist for Bcl-xL/Bcl-2, not for Mcl-1,[21] induced Bak/Bax-dependent hepatocyte apoptosis in wild-type mice but to a lesser extent in Bid KO mice. Therefore, special caution should be paid to hepatotoxicity when systemically administering a high dose of Bcl-xL–targeting molecules, because hepatocytes are suffering from Bid-mediated stresses.

In conclusion, we have demonstrated here that the BH3-only protein Bid is activated and antagonized by anti-apoptotic Bcl-2 family proteins under physiological conditions. BH3 stress or Bcl-2 addiction is not a unique characteristic of tumor cells. Even in healthy cells, cellular integrity is not controlled by a simple rheostat between Bax-like molecules and Bcl-2–like molecules. The current study reveals a previously unrecognized complicated network of Bcl-2 family proteins controlling the integrity of healthy cells. Dissection of the Bcl-2 network will be important for further understanding of liver pathophysiology.

Acknowledgment: The authors thank Abbott Laboratories for providing ABT-737.

References

1. Youle RJ, Strasser A. The BCL-2 protein family: opposing activities that mediate cell death. Nat Rev Mol Cell Biol 2008;9:47-59.
2. Korsmeyer SJ, Shutter JR, Veis DJ, Merry DE, Oltvai ZN. Bcl-2/Bax: a rheostat that regulates an anti-oxidant pathway and cell death. Semin Cancer Biol 1993;4:327-332.
3. Puthalakath H, Strasser A. Keeping killers on a tight leash: transcriptional and post-translational control of the pro-apoptotic activity of BH3-only proteins. Cell Death Differ 2002;9:505-512.
4. Willis SN, Adams JM. Life in the balance: how BH3- only proteins induce apoptosis. Curr Opin Cell Biol 2005;17:617-625.
5. Yin XM. Bid, a BH3-only multi-functional molecule, is at the cross road of life and death. Gene 2006;369:7-19.
6. Scaffidi C, Fulda S, Srinivasan A, Friesen C, Li F, Tomaselli KJ, et al. Two CD95 (APO-1/Fas) signaling pathways. EMBO J 1998;17:1675-1687.
7. Yin XM, Wang K, Gross A, Zhao Y, Zinkel S, Klocke B, et al. Bid-deficient mice are resistant to Fas-induced hepatocellular apoptosis. Nature 1999; 400:886-891.
8. Takehara T, Tatsumi T, Suzuki T, Rucker EB III, Hennighausen L, Jinushi M, et al. Hepatocyte-specific disruption of Bcl-xL leads to continuous hepatocyte apoptosis and liver fibrotic responses. Gastroenterology 2004;127:1189-1197.
9. Shindler KS, Latham CB, Roth KA. Bax deficiency prevents the increased cell death of immature neurons in bcl-x-deficient mice. J Neurosci 1997; 17:3112-3119.
10. Mason KD, Carpinelli MR, Fletcher JI, Collonge JE, Hilton AA, Ellis S, et al. Programmed anuclear cell death delimits platelet life span. Cell 2007; 128:1173-1186.
11. Wagner KU, Claudio E, Rucker EB 3rd, Riedlinger G, Broussard C, Schwartzberg PL, et al. Conditional deletion of the Bcl-x gene from erythroid cells results in hemolytic anemia and profound splenomegaly. Development 2000;127:4949-4958.
12. Takeuchi O, Fisher J, Suh H, Harada H, Malynn BA, Korsmeyer SJ. Essential role of BAX,BAK in B cell homeostasis and prevention of autoimmune disease. Proc Natl Acad Sci U S A 2005;102:11272-11277.
13. Takehara T, Hayashi N, Tatsumi T, Kanto T, Mita E, Sasaki Y, et al. Interleukin 1beta protects mice from Fas-mediated hepatocyte apoptosis and death. Gastroenterology 1999;117:661-668.
14. Wang K, Yin XM, Chao DT, Milliman CL, Korsmeyer SJ. BID: a novel BH3 domain-only death agonist. Genes Dev 1996;10:2859-2869.
15. Luo X, Budihardjo I, Zou H, Slaughter C, Wang X. Bid, a Bcl2 interacting protein, mediates cytochrome c release from mitochondria in response to activation of cell surface death receptors. Cell 1998;94:481-490.
16. Seki E, Brenner DA. Toll-like receptors and adaptor molecules in liver disease: update. HEPATOLOGY 2008;48:322-335.
17. Willis SN, Chen L, Dewson G, Wei A, Naik E, Fletcher JI, et al. Proapoptotic Bak is sequestered by Mcl-1 and Bcl-xL, but not Bcl-2, until displaced by BH3-only proteins. Genes Dev 2005;19:1129-1305.
18. Liu X, Zhu Y, Dai S, White J, Peyerl F, Kappler JW, et al. Bcl-xl does not have to bind Bax to protect T cells from death. J Exp Med 2006;203:2953-2961.
19. Kim TH, Zhao Y, Barber MJ, Kuharsky DK, Yin XM. Bid-induced cytochrome c release is mediated by a pathway independent of mitochondrial permeability transition pore and Bax. J Biol Chem 2000;275:39474-39481.
20. Adams JM, Cory S. Bcl-2-regulated apoptosis: mechanism and therapeutic potential. Curr Opin Immunol 2007;19:488-496.
21. Oltersdorf T, Elmore SW, Shoemaker AR, Armstrong RC, Augeri DJ, Belli BA, et al. An inhibitor of Bcl-2 family proteins induces regression of solid tumours. Nature 2005;435:677-681.
22. Zhang H, Nimmer PM, Tahir SK, Chen J, Fryer RM, Hahn KR, et al. Bcl-2 family proteins are essential for platelet survival. Cell Death Differ 2007;14:943-951.
23. Bouillet P, Metcalf D, Huang DCS, Tarlinton DM, Kay TWH, Köntgen F, et al. Proapoptotic Bcl-2 relative Bim required for certain apoptotic responses, leukocyte homeostasis, and to preclude autoimmunity. Science 1999;286:1735-1738.
24. Bouillet P, Cory S, Zhang LC, Strasser A, Adams JM. Degenerative disorders caused by Bcl-2 deficiency prevented by loss of its BH3-only antagonist Bim. Dev Cell 2001;1:645-653.
25. Yamada H, Tada-Oikawa S, Uchida A, Kawanishi S. TRAIL causes cleavage of bid by caspase-8 and loss of mitochondrial membrane potential resulting in apoptosis in BJAB cells. Biochem Biophys Res Commun 1999; 265:130-133.
26. Faubion WA, Guicciardi ME, Miyoshi H, Bronk SF, Roberts PJ, Svingen PA, et al. Toxic bile salts induce rodent hepatocyte apoptosis via direct activation of Fas. J Clin Invest 1999;103:137-145.
27. Takeda K, Hayakawa Y, Smyth MJ, Kayagaki N, Yamaguchi N, Kakuta S, et al. Involvement of tumor necrosis factor-related apoptosis-inducing ligand in surveillance of tumor metastasis by liver natural killer cells. Nat Med 2001;7:94-100.
28. Vick B, Weber A, Urbanik T, Maass T, Teufel A, Krammer PH, et al. Knockout of myeloid cell leukemia-1 induces liver damage and increases apoptosis susceptibility of murine hepatocytes. HEPATOLOGY 2009;49:627-636.
29. Hikita H, Takehara T, Shimizu S, Kodama T, Li W, Miyagi T, et al. Mcl-1 and Bcl-xL cooperatively maintain integrity of hepatocytes in developing and adult murine liver. HEPATOLOGY 2009; doi:10.1002/hep.23126.
30. Chipuk JE, Green DR. How do BCL-2 proteins induce mitochondrial outer membrane permeabilization? Trends Cell Biol 2008;18:157-164.
31. Takehara T, Liu X, Fujimoto J, Friedman SL, Takahashi H. Expression and role of Bcl-xL in human hepatocellular carcinomas. HEPATOLOGY 2001;34:55-61.
32. Takehara T, Takahashi H. Suppression of Bcl-xL deamidation in human hepatocellular carcinomas. Cancer Res 2003;63:3054-3057.
33. Labi V, Grespi F, Baumgartner F, Villunger A. Targeting the Bcl-2-regulated apoptosis pathway by BH3 mimetics: a breakthrough in anticancer therapy? Cell Death Differ 2008;15:977-987.
34. Mott JL, Gores GJ. Piercing the armor of hepatobiliary cancer: Bcl-2 homology domain 3 (BH3) mimetics and cell death. HEPATOLOGY 2007; 46:906-911.

＜特別寄稿＞

日本肝臓学会コンセンサス神戸2009：C型肝炎の診断と治療

西口　修平[1)*]　泉　並木[2)]　日野　啓輔[3)]　鈴木　文孝[4)]
熊田　博光[4)]　伊藤　義人[5)]　朝比奈靖浩[2)]　田守　昭博[6)]
平松　直樹[7)]　林　紀夫[7)]　工藤　正俊[8)]

索引用語：　C型慢性肝炎　診断　治療　ガイドライン

はじめに

わが国のC型肝炎の特徴は，欧米に比し高齢であり肝組織所見の進展例が多く，経過観察中に高率に肝癌が生じてくることである．このため，患者背景の異なる欧米のガイドライン[1)]はわが国では当てはまらない事項もあり，日本の患者の実態に即した独自のガイドラインの策定が必要である．このような指針を求めて，第45回日本肝臓学会総会（工藤正俊会長）において，C型肝炎（病態・診断・予後・治療）をテーマとしたコンセンサス　パネルディスカッションが開催された．すでに，第5回，第7回，第10回の日本肝臓学会大会においても，同一テーマで討議されているため，今回が4回目となる．エビデンスレベルが高く，発表者と座長のコンセンサスが得られた事項で有益な情報をInformative statementとし，推奨すべき指針をRecommendationとして取り上げた．エビデンスレベルが低いため欧米のガイドラインでは採用されていないか，発表者と座長の予備検討において全員の賛同が得られなかった事項については，アンサーパッドで学会参加者に意見を求めた．その際，回答者の2/3以上の承認が得られればConsensus Statementとして採用した．アンサーパッドの参加者は200人であり，内訳は内科医が88%，肝炎診療の経験年数が10年以上の医師が83%，肝臓学会専門医も83%を占めた．本稿では，紙面の都合でInformative statementやRecommendationは明記せず，パネルディスカッションにおいて活発な討議が行われ，結論が得られたConsensus Statementのみ全文を記載した．

1）兵庫医科大学内科学・肝胆膵科
2）武蔵野赤十字病院消化器科
3）川崎医科大学肝胆膵内科学
4）虎の門病院肝臓センター
5）京都府立医科大学消化器内科学
6）大阪市立大学肝胆膵病態内科学
7）大阪大学消化器内科学
8）近畿大学消化器内科学
*Corresponding author: nishiguc@hyo-med.ac.jp
＜受付日2009年9月16日＞＜採択日2009年9月17日＞

1）病態・診断・予後

1. C型肝炎の発症機序

C型肝炎ウイルス（HCV）の肝細胞への感染はHCV E2タンパクがCD81と結合することが必要であると報告されたが，その後scavenger receptor class B type I（SR-B1）やclaudin-1（CLDN1）といった宿主タンパクも関与することが示された．さらに2009年になってoccluding（OCLN）がHCV感染に不可欠であることが明らかとなった．興味深いことにCLDN1とOCLNはともにtight junctionに存在する分子であり，HCVが肝細胞に接着した後の細胞内への取り込みに重要であると考えられている．さらにCD81とOCLNはHCV感染の種特異性に関与する分子であることも示されている[2)]．

HCVの持続感染が成立するためには，宿主の自然免疫からの回避が必要である．最近，HCVによる自然免疫の抑制機構が明らかにされた．すなわち，複製中のHCV RNAの一部はPAMPとしてRIG-IやTLRに認識される．RIG-Iに認識されたシグナルはIPS-1を介して内因性のインターフェロン（IFN）シグナルを活性化する．産生されたIFNはIFNレセプターに結合してJak-STATシグナルを活性化してIFN応答遺伝子の発現を促す．しかし，HCV NS3/4A proteaseはIPS-1を断裂することでIFNシグナルを阻害しIFN産生を抑制する．また，HCVコアタンパクに誘導されるSOCS-3はJak-

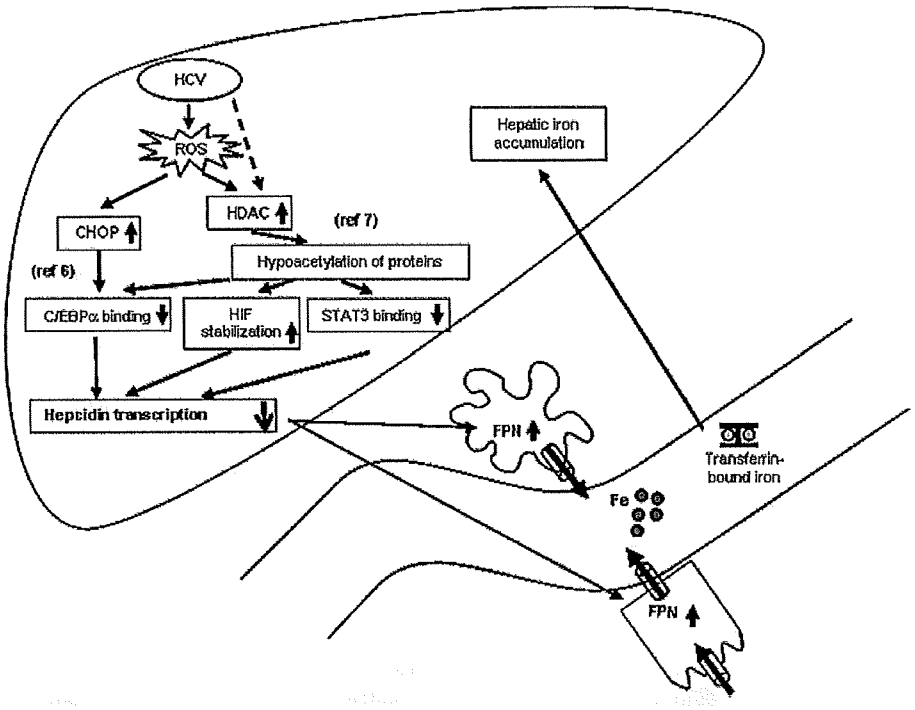

Fig. 1　Schematic diagram depicting the mechanisms underlying the hepatic iron accumulation induced by HCV
HCV-induced ROS reduces hepcidin transcription through the inhibited binding of CHOP and/or STAt3 to the hepcidin promoter, and/or stabilization of HIF that is negative hepcidin regulator.
HCV, hepatitis C virus; ROS, reactive oxygen species; HDAC, histone deacetylase; CHOP, C/EBP homology protein; C/EBP, CCAAT/enhancer-binding protein; HIF, hypoxia inducible factor; STAT, signal transducer and activation of transcription; FPN, ferroportin

STATシグナルを阻害してIFN応答遺伝子の発現を抑制し，NS5Aタンパクは IL-8の産生を亢進し，おそらくIFN応答遺伝子の発現を変化させることでIFNの抗ウイルス効果を減弱させる．更には，NS5AやE2タンパクはPKRに結合して，PKRの酵素活性を抑制することでIFNのウイルスタンパク翻訳抑制効果を阻害する[3]．HCVは以上に示したような様々な機構で宿主の自然免疫を回避すると考えられる．

HCVの持続感染成立後の肝細胞障害では，酸化ストレスが重要な役割を担っている．HCVコアタンパクはミトコンドリアを傷害し活性酸素を産生し肝臓に酸化ストレスを引き起こす[4][5]．さらにはTNFαやSOCS-3を介したinsulin receptor substrate（IRS）の抑制によるインスリン抵抗性の亢進，MTP抑制やSREBP1亢進による肝脂肪化，hepcidinの転写抑制を介した鉄蓄積などを引き起こし，C型肝炎に特徴的な病態を引き起こす（Fig. 1）[6][7]．これらの病態は肝発癌とも深く関連しており，さらにはペグインターフェロン（PEG-IFN）・リバビリン（RBV）併用療法の治療効果にも影響を与えることが報告されている．但し，肝内鉄過剰と抗ウイルス効果との関係については未だ一定の結論に至っていない．

Consensus Statement 1:

インスリン抵抗性と肝脂肪化はPEG-IFN・RBV併用療法の治療効果と関連する．(Level 2a, Grade C)

このようにC型肝炎の発症機序は次第に明らかにされつつあるが，肝発癌予測と抗ウイルス療法の効果予測に不可欠なのが肝線維化の評価である．最近ではelastographyを用いた非侵襲的な肝線維化の評価もなされているが，中等度の線維化の評価は未だ困難である．「肝線維化の評価のために肝生検は必要か？」という質

Table 1 Factors associated with sustained virological response to 48-week peginterferonribavirin combination therapy in patients infected with HCV genotype 1b, identified by multivariate analysis (n=114) [11]

Factor	Category	Risk ratio (95% confidence interval)	P
Amino acid substitution in core region	1: double wild	1	
	2: non-double wild	0.102 (0.022-0.474)	0.004
LDL cholesterol (mg/dL)	1: < 86	1	
	2: ≥ 86	12.87 (2.177-76.09)	0.005
Gender	1: male	1	
	2: female	0.091 (0.017-0.486)	0.005
ICG R15 (%)	1: < 10	1	
	2: ≥ 10	0.107 (0.017-0.678)	0.018
γ-GTP	1: < 109	1	
	2: ≥ 109	0.096 (0.0011-0.819)	0.032
Ribavirin dose (mg/kg)	1: < 11.0	1	
	2: ≥ 11.0	5.173 (1.152-23.22)	0.032

問に対して，今回のアンサーパッドの集計では74%の賛同が得られた．

Consensus Statement 2:

肝発癌や抗ウイルス療法の治療効果と関連する宿主側因子として肝組織の線維化の程度（staging）が重要であるが，stagingの評価には肝生検が推奨される．(Level 1，Grade C)

2. ウイルス変異と病態

C型肝炎の診断にはHCV RNAの測定とともに，ウイルス量，型（genotype）の測定が重要である．さらにHCV RNA遺伝子の変異について新たな知見が得られている．これらの因子はC型肝炎に対するIFN療法（RBVの併用療法を含む）の治療効果の予測に非常に重要である．ウイルス量の測定法は，2000年以降アンプリコアHCVモニター法が用いられてきたが，2007年末から高感度かつ広範囲の測定レンジをもつreal-time PCR法を用いた測定が可能となっている．このようなウイルス量とウイルスの型（genotypeまたはserotype）の測定はIFN治療の効果予測や治療中の抗ウイルス効果をみるなど臨床的な有用性が高い[8]．

ウイルスの遺伝子変異は，主としてgenotype 1b型のウイルスで多く検討されている．IFN単独投与におけるNS5A aa2209-2248 (interferon sensitivity determining region；ISDR)領域のアミノ酸変異数が治療効果に関係することが明らかになった．HCV-Jのアミノ酸配列と比較してISDRのアミノ酸変異数が多い場合，IFN単独療法でのSVR率が高いことが報告されている[9]．さらに現在治療の主体である，PEG-IFNとRBV併用療法（48週間）においてもISDRの変異数は効果予測に重要である[10]．

Table 2 Effect of the IFN treatment on the annual incidence of hepatocellular carcinoma in each fibrosis staging

	Control	IFN-treated		
		All	SVR	non-SVR
Patient's number	490	2400	789	1658
Staging				
F1	0.45%	0.08%	0.11%	0.07%
F2	1.99%	0.54%	0.10%	0.78%
F3	5.34%	1.95%	1.29%	2.20%
F4	7.88%	4.16%	0.49%	5.32%

Data were adopted from IHIT study[16]

Consensus Statement 3:

ISDRの変異は，IFN単独またはRBVとの併用療法におけるSVRに関係するので，治療前に測定すべきである．(Level 2a，Grade B)

さらに，HCV Core領域のアミノ酸置換の有無（70番目と91番目の変異）がPEG-IFNとRBV併用療法の